SEMIANNUAL REPORTS NUMBERS 13, 14, 15

and

QUARTERLY REPORT NUMBER 16

to the

NATIONAL AERONAUTICS AND SPACE ADMINISTRATION
Washington, D. C. 20546

for

GRANT NGR 33-008-009

TITLE OF RESEARCH:

Properties of Simple Atoms and Ions

PERIOD:

January 1, 1969 - September 30, 1970

SUBMITTED BY:

Columbia Astrophysics Laboratory
Department of Physics
Columbia University
New York, New York 10027

R. Novick

Principal Investigator

November, 1970

Personnel

Principal Investigator: R. Novick, Professor of Physics

L. M. Blau, Research Associate

C. Kocher, Research Physicist

C. J. Artura, J. E. Clendenin, S. H. Dworetsky, and D. Weinflash, Graduate Research Assistants, candidates for the Ph.D. degree in physics.

Degrees Awarded

C. J. Artura - Ph.D.

S. H. Dworetsky - Ph.D.

Publications

C. J. Artura, R. Novick, and N. Tolk, "Spectrum of the Two-Photon Emission from the Metastable State of Singly Ionized Helium," Ap. J. Letters 157, L181-L186 (1969).

R. Novick, "The Metastability of the $2\,^2S_{1/2}$ State of Hydrogenic Atoms," Comments on Atomic and Molecular Physics I (4), 97-103 (1969).

S. H. Dworetsky and R. Novick, "Experimental Tests of the Post-Collision-Interaction Model for the He^+ - He Excitation Functions," Phys. Rev. Letters 23, 1484-1488 (1969).

S. H. Dworetsky, R. Novick, and N. Tolk, "Total Excitation Cross Sections for the 2^1P State of He in Low-Energy He^+ - He Collisions," Sixth International Conference on the Physics of Electronic and Atomic Collisions, Massachusetts Institute of Technology, Cambridge, Massachusetts, July 28 - August 2, 1969.

R. C. Isler, S. Marcus, and R. Novick, "Fine Structure of the 3^2P and 4^2P States of Lithium," Phys. Rev. 187, 66-75 (1969).

R. C. Isler, S. Marcus, and R. Novick, "Hyperfine Structure of the 3^2P and 4^2P States of Lithium and Lifetime of the 3^2P State," Phys. Rev. 187, 76-84 (1969).

R. Novick, "Low-Energy Ion Atom Excitation," Sixth Intercenter and Contractors Conference on Plasma Physics, Langley Research Center, Hampton, Virginia, December 8-10, 1969.

L. M. Blau, R. Novick, and D. Weinflash, "Lifetimes and Fine Structure of the Metastable Autoionizing $(1s2s2p)^4P_J$ States of the Negative Helium Ion," Phys. Rev. Letters 24, 1268-1272 (1970).

R. Novick and D. Weinflash, "Precision Measurement of the Fine Structure and Lifetimes of the $(1s2s2p)^4P_J$ States of He^- and Li^*," for Proceedings of the International Conference on Precision Measurements and Fundamental Constants, National Bureau of Standards, Gaithersburg, Maryland, August 3-7, 1970 (to be published).

Description of Research

During the period reported herein, essentially all of the work has been completed concerning "Excitation in Low-Energy He^+ - He Collisions" and "Spectral Distribution of the Two-Photon Emission from the $2\ ^2S_{1/2}$ State of He^+." Published reports of this work are attached as Appendixes A and C, respectively. Work on the negative helium ion and on the precise measurement of the metastable lifetime of the 2S state of He^+ is continuing. More explicit descriptions follow.

I. EXCITATION IN LOW-ENERGY HE^+ - HE COLLISIONS

An experimental study of excitation of He I states in low-energy He^+ - He collisions was undertaken in the energy range from 5 keV down to the energy conservation thresholds. Excitation of particular He I states was observed with the use of single-photon counting techniques. The results include the observation of large low-energy cross sections, the measurement of the particular excitation thresholds which are found to lie above the energy conservation threshold, the observation of large-scale oscillatory structure in the excitation functions as the He^+ ion energy is varied, and a study of the velocity dependence of this structure. These results cannot be understood in terms of the simple application of the Massey Adiabatic Criterion. A molecular model proposed by W. Lichten does explain many of the observed phenomena but does not predict any oscillatory structure. Recent theoretical work by Rosenthal and Foley, which takes into account the multiple pseudocrossings among the various associated molecular curves, has led to a qualitative understanding of almost all of the observed phenomena.

We include in Appendix A the published reports discussing this work.

II. LIFETIMES AND FINE STRUCTURE OF METASTABLE AUTOIONIZING STATES OF THE NEGATIVE HELIUM ION

By time-of-flight techniques in an axial magnetic field, we have studied the negative ion of He^4 in the metastable autoionizing $(1s2s2p)\,^4P_J$ states.

In the experiment, a beam of He^- was prepared from a He^+ beam by double charge exchange. A 3000-eV He^+ beam was extracted from an 80-MHz rf discharge and passed through a potassium vapor where one collision produces He^* and a second collision produces the desired He^- state. The charge components of the beam were electrostatically separated, and the negative beam was directed into a 10-meter drift tube, where it was decelerated to a typical energy of 100 eV. The metastable current was detected by a Faraday cup, movable the entire length of the drift tube. A 20-volt retarding potential was applied to a high-transparency grid placed across the entrance of the detector. This excludes from the detector the electrons spontaneously produced in the beam by autoionization, so that the current received by the Faraday cup is due to He^- alone. Magnetic quenching of the metastable signal was observed at fields as low as 400 gauss. Approximate lifetimes of 500, 10, and 16 microseconds were obtained for the J = 5/2, 3/2, and 1/2 states, respectively. In addition, the $^4P_{5/2} - {}^4P_{3/2}$ fine-structure interval has been estimated to be 0.036 ± 0.009 cm^{-1} from the magnetic quenching data between 350 and 1400 gauss. Quenching of the metastable beam by residual gas in the drift tube was also observed. The quoted lifetimes against autoionization are extrapolations to zero pressure.

We are at present considering the feasibility of a very high precision measurement of radio-frequency and microwave resonances that would be of considerable theoretical interest. Our investigations indicate that the differential metastability and magnetic quenching of the ^4P_J states of He^- could be exploited to build a practical source of polarized He^3 nuclei.

Reprints of two articles describing this work are included in Appendix B.

III. SPECTRAL DISTRIBUTION OF THE TWO-PHOTON EMISSION FROM THE $2\ ^2S_{1/2}$ STATE OF HE^+

Completed in the spring of 1969 was an experimental verification of the spectral distribution of the two-photon emission from the metastable $2\ ^2S_{1/2}$ state of He^+. A broadband spectroscopic coincidence counting technique was employed. The spectral distribution of the two-photon decay of metastable He^+ was studied by observing the coincidences between a "hard" uv phototube (sensitive from 200 to 1200 Å) and a "soft" uv phototube (sensitive from 1050 to 3500 Å) preceded by various broadband filters. Two-photon coincidence counting rates were observed experimentally and agree with those calculated from the theoretically predicted spectral distribution of the two-photon emission. Furthermore, the theoretically null "soft" - "soft" coincidence counting rate was shown to be less than 0.04 counts per minute. This is a factor of 150 smaller than either the "hard" - "hard" or "hard" - "soft" coincidence counting rate, each of which is typically six counts per minute. In addition, radiation due to the impact of low-energy metastable singly ionized helium on helium and on the other rare gases was detected. This is the first experimental study of very low-energy ion-atom excitation processes where one of the collision partners is initially in an excited state.

In Appendix C we include a reprint of our publication of these results.

IV. TWO-PHOTON DECAY OF THE 2 $^2S_{1/2}$ STATE OF HE^+

Upon completion of the photon coincidence observations, the experiment to observe the decay in flight of metastable helium ions was resumed. Construction of the experimental apparatus for the precise measurement of the metastable lifetime is nearing completion.

A beam of He^+ ions in the 2S state is produced by electron bombardment. We have improved the excitation source through the use of helium gas of extremely high purity (contamination less than 1 part in 10^6) and the replacement of the original oxide-coated cathode by a porous tungsten dispenser cathode.

Detection of the 2S ions is accomplished by the use of a surface Auger detector in conjunction with modulation of the beam at the Lamb-shift frequency (14 GHz). The detector records a signal due to the differential secondary electron emission between the 1S and 2S states. A solid-state square-wave modulator operating at low frequency has been constructed for the control of a klystron tuned to the Lamb-shift frequency. The klystron is coupled to a microwave cavity through which the helium ion beam passes and in which the 2S component of the beam is quenched to the ground state.

The ac signal corresponding to 2S quenching has been observed. The detector used in these tests was mounted in a fixed position, separated from the excitation source by a system of electrostatic lenses. After amplification by a varactor bridge operational amplifier, the ac signal is fed into a lock-in amplifier. The output from the lock-in amplifier is plotted on the accompanying graph as a function of source bombarding voltage. It shows clearly the 65-eV threshold for the production of metastable ions. The signal intensity indicates that metastables constitute nearly 1% of the total beam; the remainder are ground-state ions.

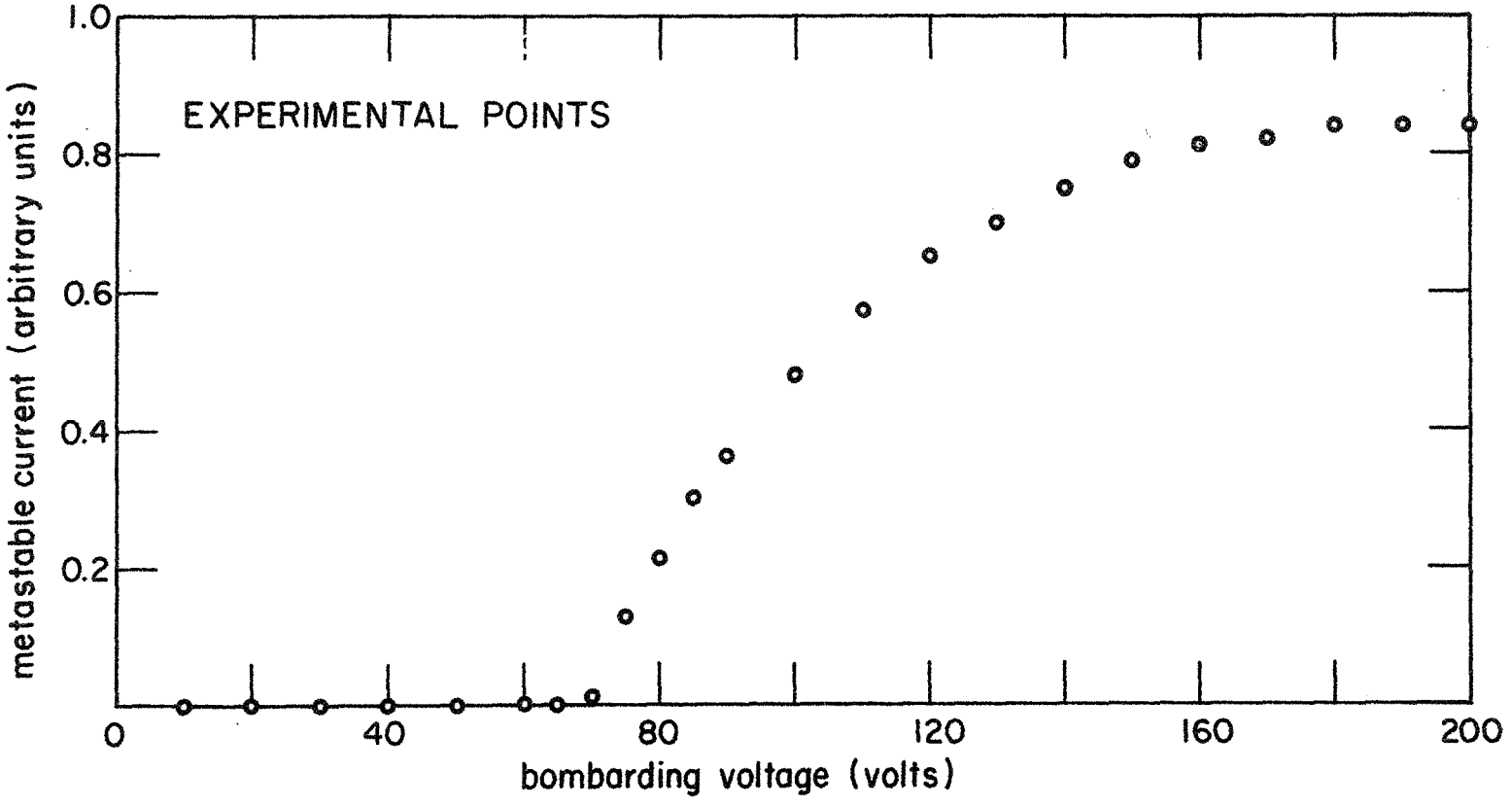
EXPERIMENTAL POINTS
metastable current (arbitrary units)
1.0
0.8
0.6
0.4
0.2
0
40
80
120
160
200
bombarding voltage (volts)

The theoretically predicted lifetime of the 2S state is 2×10^{-3} seconds. With a beam velocity of the order of 10^6 cm/sec, a drift tube several meters in length is necessary for a precise measurement of the lifetime. For this purpose a stainless-steel drift tube, 24 cm in diameter and 9 meters in length, was constructed and is awaiting installation. A gate valve inserted between the source and the drift tube permits the source cathode to be replaced without the loss of vacuum in the drift tube. By moving the detector along the beam, the decay of the 2S state will be observed. The transport mechanism for the detector is nearing completion in our shops. It consists of a platform sliding on stainless-steel rails and driven by an externally powered chain-and-sprocket drive.

We hope to complete the major construction of the apparatus within two months and to obtain a preliminary measurement of the 2S lifetime later this winter.

APPENDIXES

A. S. H. Dworetsky, R. Novick, and N. Tolk, "Total Excitation Cross Sections for the 2 ^1P State of He in Low-Energy He^+ - He Collisions," Sixth International Conference on the Physics of Electronic and Atomic Collisions, Massachusetts Institute of Technology, Cambridge, Massachusetts, July 28 - August 2, 1969.

S. H. Dworetsky and R. Novick, "Experimental Tests of the Post-Collision-Interaction Model for the He^+ - He Excitation Functions," Phys. Rev. Letters 23, 1484-1488 (29 December 1969).

B. L. M. Blau, R. Novick, and D. Weinflash, "Lifetimes and Fine Structure of the Metastable Autoionizing $(1s2s2p)\,^4P_J$ States of the Negative Helium Ion," Phys. Rev. Letters 24, 1268-1272 (8 June 1970).

R. Novick and D. Weinflash, "Precision Measurement of the Fine Structure and Lifetimes of the $(1s2s2p)\,^4P_J$ States of He^- and Li^*," for Proceedings of the International Conference on Precision Measurements and Fundamental Constants, National Bureau of Standards, Gaithersburg, Maryland, August 3 - 7, 1970.

C. C. J. Artura, N. Tolk, and R. Novick, "Spectrum of the Two-Photon Emission from the Metastable State of Singly Ionized Helium," Ap. J. 157, L181-L186 (September 1969).

Total Excitation Cross Sections for the 2^1P State of He in Low-Energy He^+ - He Collisions

S. H. Dworetsky, R. Novick, and N. Tolk

Columbia Radiation Laboratory, Department of Physics,
Columbia University, New York, New York 10027

Submitted to

6th International Conference on the Physics
of Electronic and Atomic Collisions
Massachusetts Institute of Technology, July 1969

March 1969

Total Excitation Cross Sections for the 2^1P State of He in Low-Energy He^+ - He Collisions*

S. H. Dworetsky, R. Novick†, and N. Tolk††

Columbia Radiation Laboratory, Department of Physics,
Columbia University, New York, New York 10027

The total cross section has been observed for the 584-Å (2^1P-1^1S) line in low-energy He^+ - He collisions (50 eV - 2500 eV). Previously the 10,830-Å (2^3P-2^3S) He line was observed in the same energy region.[1] The observed excitation functions (Figs. 1 and 2) do not exhibit any oscillatory structure. Previously reported data[2] for the excitation of lines originating in the n = 3, 4, and 5 states of He showed many instances of strong oscillatory structure. The present and previously reported data will be compared with existing differential cross-section data for excitation of the 2^3S state of He with 600 eV He^+ ions.[4] These data exhibit strong oscillatory structure as a function of scattering angle. The presence or absence of structure in these differential and total inelastic cross-section data can be explained in terms of molecular potential-energy curve crossings. The previously invoked model,[2-4] which contained one ground-state crossing at $R \approx 1$Å, is sufficient to explain the structure in the differential cross-section data. However, to understand the absence or presence of structure in the total cross-section data, one must invoke a recently proposed model which includes an excited state crossing at $R \approx 15$Å.[5]

The present work was undertaken as part of a continuing effort to understand low-energy He^+ - He collisions in terms of molecular potential-energy curves. In the case of the higher excited states ($n \geq 3$), the multiplicity and proximity of levels greatly complicates the problem and makes it difficult to assess the validity of any theoretical model. However, the $n = 2$ levels are well separated from the higher levels and are therefore more amenable to critical theoretical analysis. A concerted effort was therefore initiated to obtain excitation functions for the 2P states of He.

Previous data for inelastic low-energy He^+ - He collisions had been analyzed in terms of a single curve crossing which was shown to exist at about $R_I = 1\text{Å}$. At this value of internuclear separation, the ground-state curve crosses a number of excited-state curves. Such a crossing is responsible for the population of various excited states at values of bombarding energy which are very much lower than those predicted on the basis of a simple application of the adiabatic criterion.

It was felt that structure observed in the various inelastic He^+ - He collisions was due to coherent phase development when $R < R_I$. In this region the system evolves as a quantum mechanical superposition of at least two possible states. Each develops phase consistent with its energy. The phase difference thus acquired yields an interference phenomenon when the states mix again during the second, outward bound passage of the crossing. It has been shown that this phase difference is strongly dependent on the impact parameter $\underline{b}$ and hence on scattering angle θ. While

this phenomenon is capable of furnishing an adequate explanation of the oscillatory structure in the differential cross-section data, it fails to explain the structure in the total cross-section data. The strong $\underline{b}$ dependence of the acquired phase difference results in no energy-dependent structure when one integrates over $\underline{b}$ to obtain the total cross section.

To explain the structure in the total cross-section data, it has been suggested, and shown, that in addition to the inner crossing, an outer crossing between two excited potential-energy curves exists at $R \approx 7 - 15\text{Å}$.[5] The two excited states are initially populated at the inner crossing. When $R_0 > R > R_I$, each excited state develops phase at a rate consistent with its energy. A phase difference develops and inteference results at the outer crossing R_0. The phase difference in the final state interaction is not strongly $\underline{b}$ dependent, and the structure persists in the total cross sections. The absence of strong $\underline{b}$ dependence implies that the structure in the differential cross-section data is unaffected by the outer crossing and is still explained in terms of the inner crossing.

Whereas outer crossings between excited states exist for the $n = 3, 4, 5$, and higher levels, it has been shown theoretically that no outer crossing exists for the excited 2P states. It was, therefore, predicted that no oscillatory structure would be observed in the excitation of the 2P states. This is, in fact, borne out by the data presented here. While the outer crossing is responsible for the oscillatory structure of the higher excited states ($n \geq 3$), in all cases the excitation threshold is determined

by the location of the inner crossing. This threshold has been measured for the 10,830-Å transition and is consistent with the existent calculations. Low signal levels precluded the measurement of the threshold for the 584-Å transition.

Our apparatus includes a He^+ electron-bombardment source.[6] An oxide-coated cathode yields an electron current of 500 mA or greater. By maintaining the electron-bombarding voltage below 55 eV, we can be sure of a pure ground-state He^+ beam free of metastable 2S ions.

Excitation is observed by single-photon counting of the emitted light when the excited states decay. A suitable filter was used to isolate the 10,830-Å light, and this infrared radiation was detected with an EMI S-1 phototube, cooled with liquid nitrogen. The net signal was the difference between counts observed with and without target gas in the chamber. By using a standard lamp for intensity calibration and by observing the 3^3S-2^3P and 3^3D-2^3P transitions, it was concluded that cascading accounts for less than 10% of the 10,830-Å signal.

Observation of the 584-Å transition presents considerably more difficulty. Since no filters exist for 584-Å radiation, we used a McPherson model 220 vacuum ultraviolet 1-meter normal-incidence grating spectrometer to isolate this line. The large f number of this instrument reduces the signal considerably. We used a platinum-coated grating blazed at 800-Å to improve reflectance. An EMI 9603 open-face multiplier was used as a detector. Both the photomultiplier chamber and the vacuum chamber coupling the spectrometer to the target chamber were evacuated with oil diffusion pumps (see Fig. 5).

In an attempt to observe resonance transitions such as the He I 584-Å line, a careful analysis of the problem of resonance trapping is required. In addition to reabsorption of the resonant radiation, one must take into account the finite branching ratio (0.001) between the (2^1P-2^1S) and (2^1P-1^1S) transition. If many reabsorptions occur, even this small ratio will result in loss of 584-Å radiation to the 20,581-Å transition. A simple calculation, however, shows that because of momentum transfer in the excitation process, most of the 584-Å radiation is shifted sufficiently to prevent its absorption. The result is that there are very few reabsorptions of the resonance radiation. However, since the path length through the spectrometer is 2 meters, and since the spectrometer is vacuum coupled to the relatively high pressure of the target chamber, a collodion window was added to separate the spectrometer and target chambers. This avoids all trapping which might occur during the passage of light through the spectrometer.

Two specific experimental tests were performed to insure that there was no trapping. First, measurements of signal versus pressure yielded a straight line, which is to be expected only if trapping is negligible. Second, He^3 was used as a target particle, which provided an isotope shift large enough to prevent reabsorption of radiation emitted from a He^4 atom. No change in signal strength or energy dependence was observed in these isotopic experiments, thereby confirming the absence of trapping effects.

The 584-Å data are shown in Fig. 1. There is a shoulder in the 584-Å data at $\approx$ 200 eV and a possible indication of a shoulder at $\approx$ 100 eV. Likewise there is a conspicuous shoulder in the 10,830-Å data at $\approx$ 110 eV (Fig. 2). If we interpret these shoulders as arising from a weak oscillatory structure superimposed on a smooth excitation function, then we find that the 584-Å and 10,830-Å oscillations are in antiphase. It is suggested that such oscillations may arise from the coherent excitation of the 2^1P and 2^3P states. The background counting rate in the 584-Å work was about 1/2 count/sec, while the signal was about 3 counts/sec at 1 keV.

The work presented here indicates that despite the complexity involved in collisional cross sections, relatively simple models serve surprisingly well to explain the existing data. In the development of these models, the lower-lying states are of greatest interest because of their isolation. Such results can be more readily discussed theoretically, and the stimulation thus provided can lead to a better understanding of more complicated problems.

References

*This work was supported in part by the Joint Services Electronics Program (U.S. Army, U.S. Navy, and U.S. Air Force) under Contract DA-28-043 AMC-00099(E), in part by the National Aeronautics and Space Administration under Grant NGR 33-008-009, and in part by the Office of Naval Research under Contract N00014-67-A-0108-0002.

†Alfred P. Sloan Research Fellow.

††Present Address: Bell Telephone Laboratories, Inc., Whippany, New Jersey.

1. Columbia Radiation Lab. Progr. Rep. No. 16, October 31, 1967, p. 33; the results from this report are to be published.

2. S. Dworetsky, R. Novick, W. W. Smith, and N. Tolk, Phys. Rev. Letters 18, 939 (1967).

3. W. Lichten, Phys. Rev. 131, 229 (1963).

4. D. C. Lorents, W. Aberth, and V. W. Hesterman, Phys. Rev. Letters 17, 849 (1966).

5. H. Rosenthal, private communication.

6. S. Dworetsky, R. Novick, W. W. Smith, and N. Tolk, Rev. Sci. Instr. 39, 1721 (1968).

Figure Captions

Figure 1: Cross section for the $2^1P - 2^1S$ transition vs energy in the laboratory system.

Figure 2: Cross section for the $2^3P - 2^3S$ transition vs energy in the laboratory system.

Figure 3: Experimental apparatus for detection of 584-Å radiation in low-energy $He^+ - He$ collisions.

1) Source chamber; 2) He^+ source; 3) intermediate pumping chamber with differential pumping slits and electrostatic ion lenses; 4) mercury diffusion pumps; 5) oil diffusion pumps; 6) spectrometer; 7) grating; 8) detector vacuum chamber; 9) photomultiplier; 10) beam detector; 11) collodion film; 12) target chamber; 13) He^+ beam; 14) path of 584-Å radiation; 15) differential pumping chamber.

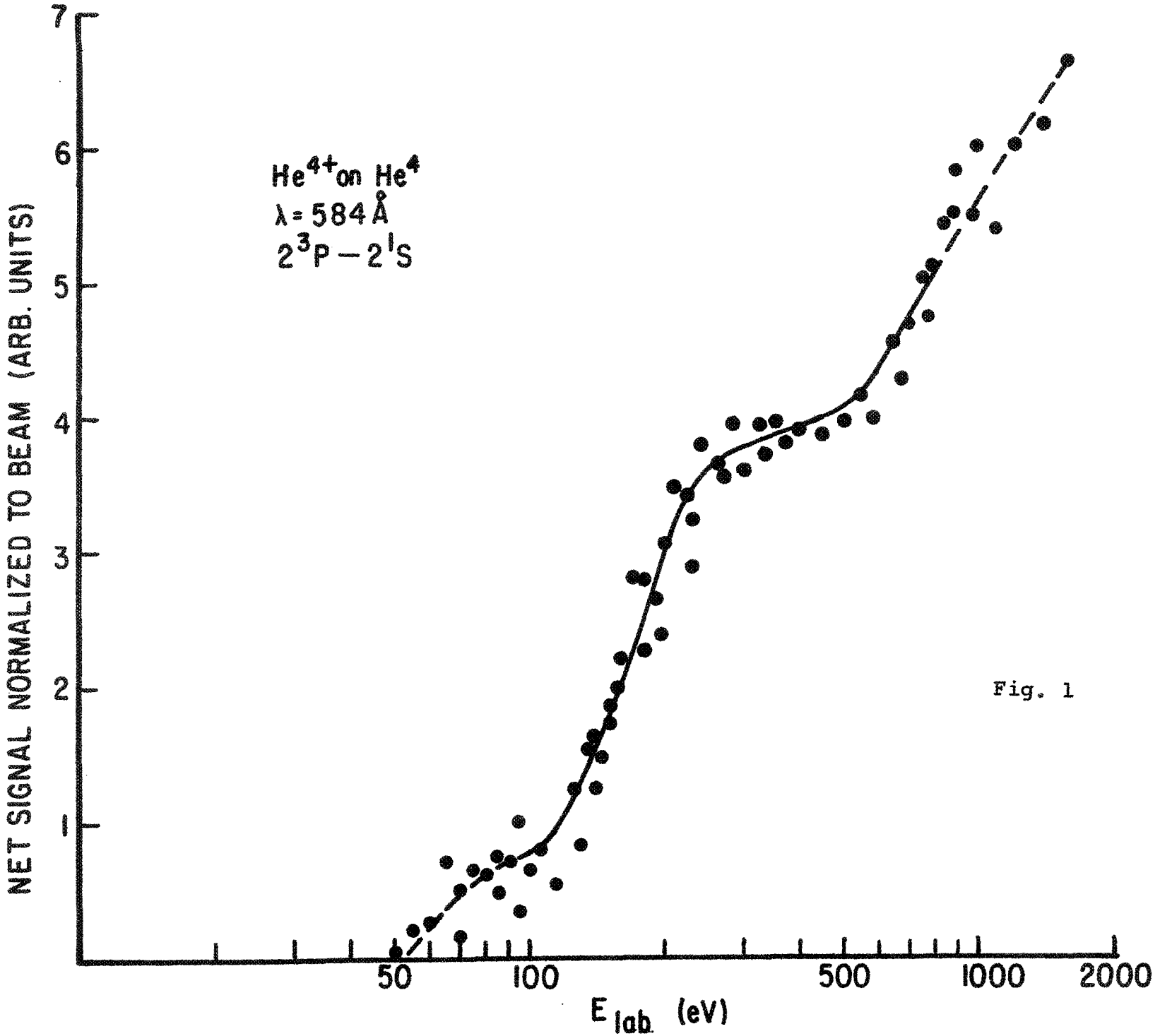
He^{4+} on He^4
λ = 584 Å
$2^3P - 2^1S$
NET SIGNAL NORMALIZED TO BEAM (ARB. UNITS)
1
2
3
4
5
6
7
50
100
500
1000
2000
E_{lab} (eV)

Fig. 1

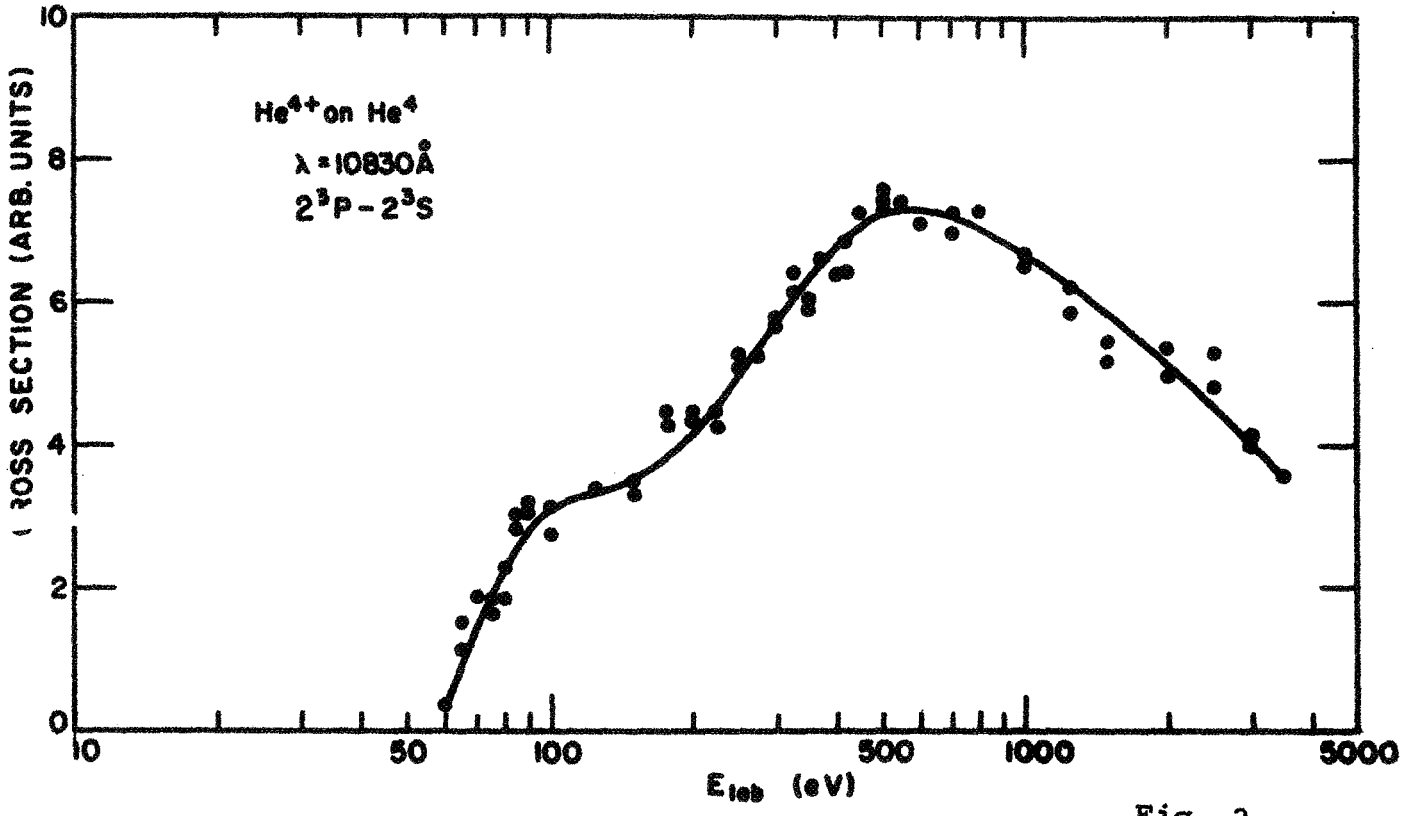
He4+on He4
λ=10830Å
2³P-2³S
CROSS SECTION (ARB. UNITS)
0
2
4
6
8
10
10
50
100
500
1000
5000
Elab (eV)

Fig. 2

Fig. 3

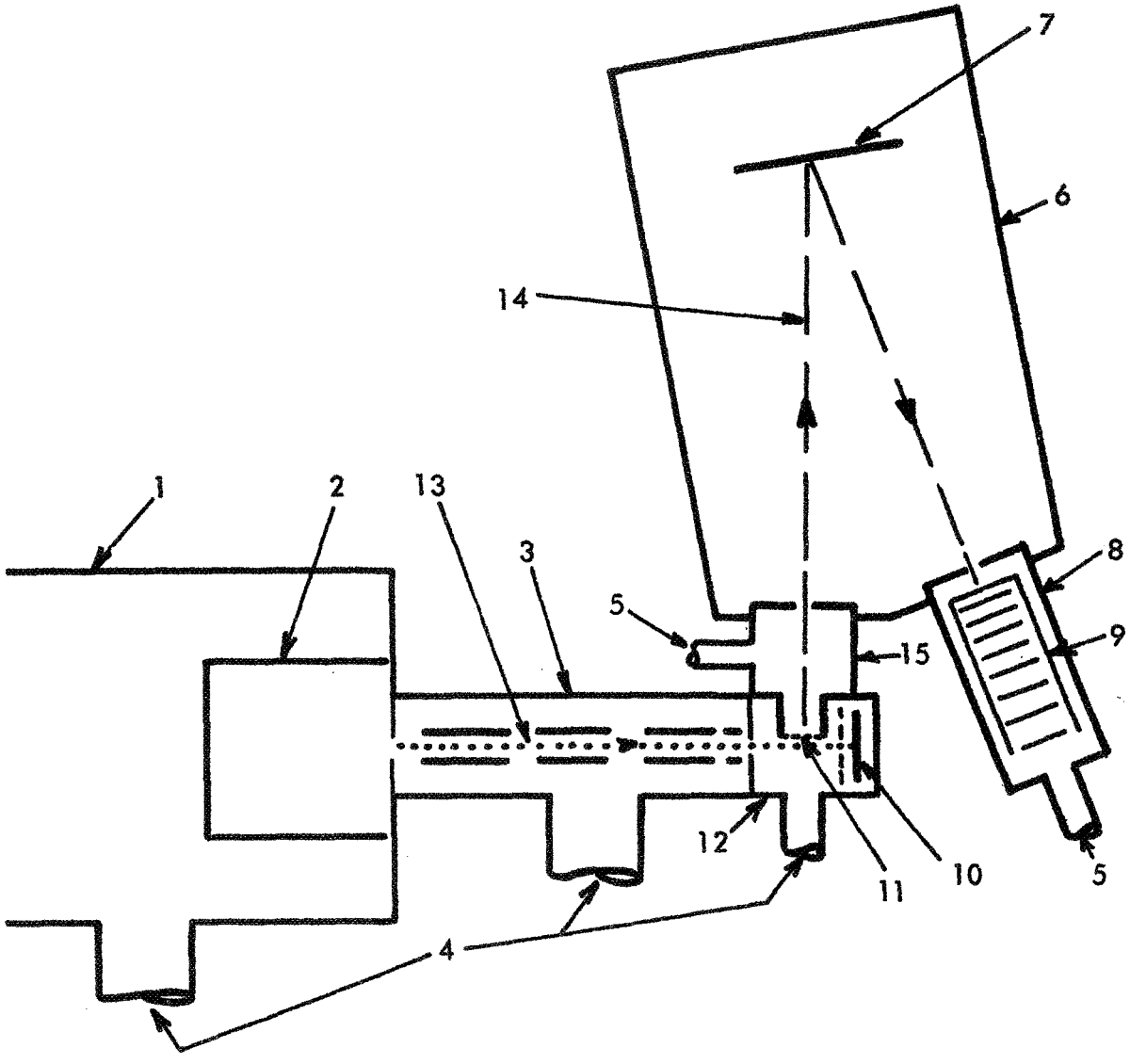

Experimental Tests of the Post-Collision-Interaction Model For the He^+ - He Excitation Functions*

by

S. H. Dworetsky

Columbia Radiation Laboratory

and

R. Novick†

Columbia Astrophysics Laboratory

Columbia University, New York, New York 10027

ABSTRACT

New data on the excitation of helium by low-energy helium ions have been obtained that provide strong support for the post-collision-interaction model proposed by Rosenthal and Foley in a companion paper. Certain details of the results that are not presently predicted by the theory are pointed out.

---

*This work was supported in part by the Joint Services Electronics Program (U. S. Army, U. S. Navy, and U. S. Air Force) under Contract DA-28-043 AMC-00099 (E), in part by the National Aeronautics and Space Administration under Grant NGR 33-008-009, and in part by the Office of Naval Research under Contract N00014-67-A-0108-0002. It is Columbia Astrophysics Laboratory Contribution No. 11.

†Alfred P. Sloan Research Fellow.

New experimental studies of low-energy He^+ - He total excitation cross sections are presented that provide strong support for a post-collision interaction model proposed by Rosenthal and Foley in a companion paper[1] (hereafter referred to as the R-F model).

We previously reported the excitation of various neutral states of He in low-energy He^+ - He collisions.[2] Two striking results of these observations were the large value of the cross section at low energies with thresholds slightly above the final state energies, and the strong oscillatory dependence of the cross sections on projectile energy. These phenomena were interpreted in terms of the molecular-potential energy curves of the He_2^+ system. To understand the low-energy excitation it was noted that, in the diabatic approximation, the gerade ground term is repulsive and pseudocrosses all of the excited state terms.[3] These pseudocrossings occur at a value of internuclear separation, R_I, of about 1 a.u. In the course of collisions with small enough impact parameters, the internuclear separation decreases and passes through R_I. As the system passes through the pseudocrossing, excitation occurs by the mechanism discussed by Landau, Zener, and Stuckelberg.[4] This accounts for the large cross section at low energies. Since the thresholds occur slightly above the final state energies, they provide a direct measure of the energy location of the pseudocrossing.[5] In addition to other results discussed here, we report new precise values for these energies which can be compared with specific molecular models.

Previously we proposed that the oscillations were produced by an interference effect which arose from the double passage of the system through the crossing at R_I. However, it has now been shown (cf. R-F)

that any phase difference thus developed is strongly dependent on the impact parameter b; consequently, the integration over impact parameters required to obtain total cross sections averages out this interference effect. Such a phase difference might contribute to the oscillations reported in differential inelastic cross sections[6] but cannot explain the structure observed in the total cross-section data.

In the companion paper, Rosenthal and Foley show that in addition to the crossing between the ground state and excited state curves at R_I, other crossings between two or more excited states exist at relatively large values of internuclear separation, $R_o \approx 20$ a.u. In this model the excitation mechanism is essentially identical with that previously considered and hence the large cross sections at low energies, and the threshold energies, are explained as before. However, the oscillations are now considered to arise when two excited states populated at R_I develop a phase difference between R_I and R_o before mixing again at R_o. Since the resulting phase difference is weakly "b"-dependent, it manifests itself in the form of oscillatory structure in the total cross section. Rosenthal and Foley show that their model correctly predicts the oscillatory structure in the excitation functions of the 3^3S and 3^1S states, and, moreover, they predict that these oscillations should be in antiphase as is in fact observed.[2] New experiments whose results strongly substantiate the R-F model are described in this paper.

Rosenthal and Foley find that in their model, outer crossings, which can efficiently mix the excited state amplitudes, exist in the $n = 3$, 4, and higher states but not in the $n = 2$ states. Hence they predict oscillatory structure in the $n = 3$ and higher excitation functions but not in the $n = 2$ cross sections. In our earlier work we observe

the n = 3, 4, and 5 levels and found strong oscillations. A new experimental study has now been made of the 584-Å line ($2^1P - 1^1S$) and 10,830-Å line ($2^3P - 2^3S$) to test the predictions of the R-F model. The apparatus was essentially the same as that used earlier except that in the case of the 10,830-Å line a liquid-nitrogen-cooled EMI No. 9684B phototube was used to detect the radiation, and the line was isolated with an interference filter. Since no filter material exists for the 584-Å light, a McPherson Model 220 uv spectrometer was used to isolate this line. The spectrometer viewed the bombarding chamber at an angle of 90° relative to the beam, and the light, after passing through the spectrometer, was detected with an EMI 9603 particle multiplier. Although resonance trapping was initially considered to be a serious problem for the 584-Å line, simple estimates indicate that the transverse momentum transferred in the course of the collision is sufficiently large so that no trapping occurs. The resulting Doppler shift, at energies greater than 100 eV and for scattering angles greater than 1°, is larger than the thermal Doppler width of the line and little absorption occurs. The possibility of trapping is further reduced by the fact that the collision region is viewed over an angular region of at least ±3° and therefore the component of velocity in the direction of viewing is sufficiently large to insure a Doppler shift greater than the thermal Doppler width. The absence of trapping was tested experimentally by observing that the pressure dependence of the signal was linear and by comparing the signal for $^3He^+ - {}^4He$ and $^4He^+ - {}^4He$ collisions. Since the $^3He - {}^4He$ isotope shift is larger than the thermal Doppler width, any possible trapping would be seriously modified by changing isotopes; yet no difference in either signal strength or the form of the excitation function was observed, confirming the absence of trapping.

The 2P excitation functions are shown in Fig. 1A. In accordance with the R-F model and unlike the n = 3, 4, and 5 excitation functions, no large-scale oscillatory structure is observed. Some small-scale structure which does appear is discussed below. The fact, noted above, that there is no significant difference between the 584-Å excitation function for $^4He^+ - ^4He$ and $^3He^+ - ^4He$ collisions shows that nuclear symmetry is not important in these phenomena.

As mentioned previously, measurement of the excitation function threshold gives an accurate value of the energy location of the inner pseudocrossing.[5] Careful measurements were made of the signal near the threshold for nine transitions. In extracting threshold values from these data, a linear threshold law was assumed in accordance with the observed steep nature of the onsets. In these experiments two phototubes were used simultaneously, one with a 3888-Å filter and the other with a filter chosen to isolate the line under study. In this way the thresholds could be obtained relative to the 3888-Å threshold. This technique was employed since there was evidence that the true beam energy differed by one or two eV from the applied potential. Such differences would be expected to arise from contact potentials, space charge effects, and surface charging. Since these effects may vary with time and operating conditions, the comparison method was employed so as to obtain the best possible values for the difference in the thresholds. It is estimated that the differences were obtained to ± 0.2 eV. The correction needed for obtaining the absolute value of the 3888-Å threshold was determined by measuring the $^3He^+ - ^4He$ and $^4He^+ - ^4He$ thresholds for this line and using

the fact that the center-of-mass threshold for these two collision combinations should be identical. In this way the energy correction at the time these data were taken and the absolute value of the 3888-Å threshold were found to be -0.63 ± 1.56 eV and 60.50 ± 1.56 eV respectively. The threshold values in the center-of-mass system and energies of the final states of the free atom are given in Table I.

The displacement of the thresholds above the final state energies of the free atom indicates that the pseudocrossing at R_I occurs above the final state energy. The observation of distinct thresholds for two excited states which cross at a large value of internuclear separation R_o (e.g., 3^3S, 3^1S) allows us to make a qualitative statement concerning the transition probability at this outer crossing at low energies. If the transition probability at this crossing were large we would expect population of the upper state at R_o even though the energy were so low that only the lower state was populated at the inner crossing. This would result in identical thresholds for both the states. The observation of distinct thresholds for these two states indicates that at low velocities the crossing at R_o is essentially adiabatic. We are thus free to interpret the thresholds as a measure of the energy location of the inner crossings.

We studied the velocity dependence of the oscillatory structure observed in a number of excitation functions by using ^3He and ^4He in various collisional combinations. For a given energy these different collisional combinations have different relative velocities. Since we believe that the oscillations are due to a phase-interference phenomenon, we scaled the cross sections according

to phase-development time by plotting the isotopic data for excitation of a given state of He versus the relative velocity at infinite internuclear separation, $v(\infty)$,

$$v(\infty) = \left[\frac{2E_L}{m_p}\right]^{1/2} = \left[\frac{2E_{c.m.}}{\mu}\right]^{1/2} \qquad (1)$$

where μ is the reduced mass of the system, E_L and $E_{c.m.}$ are the energies in the laboratory and center-of-mass frame respectively, and m_p is the mass of the projectile particle.

When the cross sections are scaled according to Eq. (1), the high-energy peaks overlap, in accordance with the assumption of a phase-interference effect. The lack of overlap at low energies (Fig. 2A) is due to the difference between the true velocity and $v(\infty)$ in this energy domain. This difference arises from the effect of the interatomic potential $V(R)$ and the centrifugal barrier b^2/R^2. In considering b^2/R^2 we note that, for excitation to occur, b must be less than R_I. Yet in the R-F model, the region of relevant phase development varies between internuclear separations of R_I, and R_o, which is of the order of 20 R_I. Therefore, in this region the value of b^2/R^2 lies between 1 and 4×10^{-3}. In view of this we neglected the centrifugal barrier in scaling the oscillations versus velocity. The effective velocity in the region of phase development is then given by

$$V(R) = \left[\frac{2}{\mu}\left(E_{c.m.} - \langle V(R)\rangle\right)\right]^{1/2} . \qquad (2)$$

Since in the model being considered the phase difference develops in the final state, we may take the average interatomic potential energy $\langle V(R)\rangle$ equal to the final state energy E_f. In

the case of the 4^3S level, the final state energy is about 23 eV and this produces a substantial modification of the velocity at low bombarding energy. The isotopic data are plotted in Fig. 2B with the velocity given by Eq. (2) with $\langle V(R) \rangle$ = 23 eV. In this plot the structure overlaps over the entire energy range in accordance with the R-F model and the above discussion.

Two experimental results remain for which only tentative explanations exist. In carefully studying the threshold behavior of the various excitation functions, we find that additional structure appears in the 4713-Å and the 3888-Å line near threshold when the ^4He - ^4He system is studied (Fig. 1B). This structure does not appear for other collisional combinations. The difference in structure appearing in the isotopic data can be explained in terms of the phase development time. As the energy decreases from the kV range, and with it the velocity, more phase difference is developed and more oscillations appear. Near threshold the velocity in the 4-4 case reaches smaller values than that in the 4-3 case. Therefore, near threshold, the 4-4 system spends more time developing phase than the 4-3 system. The data indicate that enough additional time is spent for one more oscillation to appear. In the case of differential scattering experiments it is observed that the data obtained in collisions with identical isotopes, i.e., ^3He - ^3He and ^4He - ^4He, exhibit more structure than in the case of the unsymmetric nuclear collisions ^3He - ^4He. This additional structure is attributed to the effects of nuclear symmetry. In the present case, in order to rule out this possibility, we performed an experiment in which we used ^3He ions on ^3He. The results obtained in this

experiment did not show the additional structure seen in the $^4He - ^4He$ case, and we conclude that nuclear symmetry is not responsible for the extra oscillation shown in Fig. 1B.

One additional unexplained experimental result involves the shoulders observed near threshold in the 2P excitation functions (Fig. 1A). If one interprets these features as low-amplitude oscillations superimposed on a smooth excitation curve, then the oscillations in the 2^1P and 2^3P excitation functions are in apparent antiphase. This result seems to indicate that some small mixing occurs between these states although, as previously mentioned, these states are not coupled through an outer crossing. No theoretical interpretation of this result is as yet available. However, we would like to suggest that this effect may result from a residual interference effect arising at the inner crossing.[2]

The results presented here have stimulated considerable efforts to understand the detailed interactions occuring in low-energy ion-atom collisions. The theory recently developed by Rosenthal and Foley has been remarkably successful in leading to an understanding of those results. Some unanswered questions remain, however, and further theoretical efforts will be needed to answer them. It is clear that the full elucidation of the detailed structure of the excitation functions will provide a powerful test of our understanding of the dynamics of the unbound molecular state formed during these inelastic conditions.

The authors are most indebted to Professor W.W. Smith and Dr. N. Tolk for their extensive aid in obtaining these results and in discussing their interpretation. We are also indebted to Dr. H. Foley and Mr. H. Rosenthal for extensive discussions on their new

theoretical model. This work would not have been possible without the enthusiastic support of the members of the Physics Department Machine Shop and Electronics Shop.

REFERENCES

1. Cf. preceding paper in this volume by H. Rosenthal and H. Foley.

2. S. Dworetsky, R. Novick, N. Tolk, and W. W. Smith, Phys. Rev. Letters 18, 939 (1967).

3. W. Lichten, Phys. Rev. 131, 229 (1963).

4. L. Landau, Physik. Z. Sowjet. 2, 46 (1932).

C. Zener, Proc. Roy. Soc. (London) A137, 696 (1932).

E. C. G. Stuckelberg, Helv. Phys. Acts 5, 370 (1932).

5. This statement is subject to a discussion which follows.

6. D. C. Lorents, W. Aberth, and V. W. Hesterman, Phys. Rev. Letters 17, 849 (1967).

7. W. Aberth, D. C. Lorents, R. P. Marchi, and F. T. Smith, Phys. Rev. Letters 14, 776 (1965).

FIGURE CAPTIONS

Fig. 1. (A) Cross sections for the excitation of the 2P states of He in He^+ - He collisions. (B) Detailed threshold behavior of the 3888-Å excitation function for $^4He^+$ - ^4He and $^3He^+$ - ^4He collisions.

Fig. 2. (A) Excitation cross section for the 4713-Å He I line in $^4He^+$ - ^4He and $^4He^+$ - ^3He collisions plotted versus relative velocity at infinite internuclear separation, $v(\infty)$. (B) Excitation cross section for the 4713-Å He I line in $^4He^+$ - ^4He and $^4He^+$ - ^3He collisions plotted versus relative velocity in the final state.

Table I. Thresholds for Excitation of Excited He I States

State	Threshold Relative to 3^3P (Lab.eV)[a]	Absolute Threshold (c.m. eV)[b]	Difference between the Threshold and Final State Energies (c.m. eV)[c]
2^3P	-7.30	26.60	5.64
3^3S	-2.57	28.97	6.26
3^1S	-1.85	29.33	6.42
3^1D	-0.40	30.05	6.98
3^3P	-	30.25	7.25
3^3D	+0.10	30.30	7.23
3^1P	+1.80	31.15	8.07
4^3S	+1.87	31.18	7.59
5^3S	+2.70	31.60	7.63

[a]These energy differences are measured in the laboratory system and are believed to be reliable to ± 0.2 eV.

[b]The energy of the 3^3P threshold is 60.50 ± 1.56 eV (lab system). The other values in this column (col.3) are obtained using the absolute 3^3P threshold and the values in col. 2. Hence, the absolute values in col. 3 are reliable to ± 0.78 eV (c.m. system). However, the differences in the values in col. 3 are reliable to ± 0.10 (c.m.) as are those in col. 2 from which they are derived.

[c]As in col. 3, these values are reliable to ± 0.78 eV (c.m.) and their differences are reliable to ± 0.10 eV (c.m.).

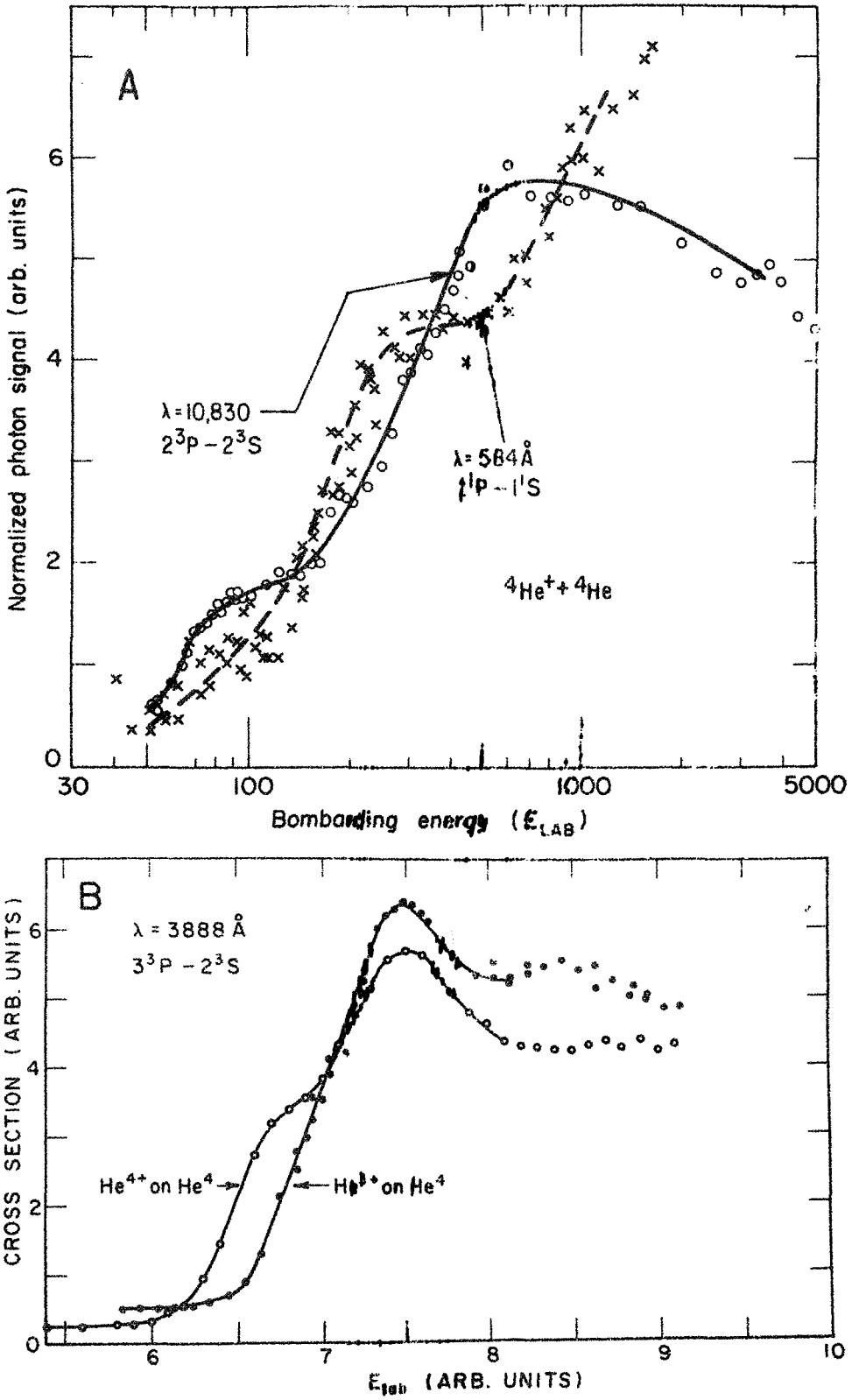

Fig. 1. (A) Cross sections for the excitation of the 2P states of He in He^+ - He collisions. (B) Detailed threshold behavior of the 3888-Å excitation function for $^4He^+$ - ^4He and $^3He^+$ - ^4He collisions.

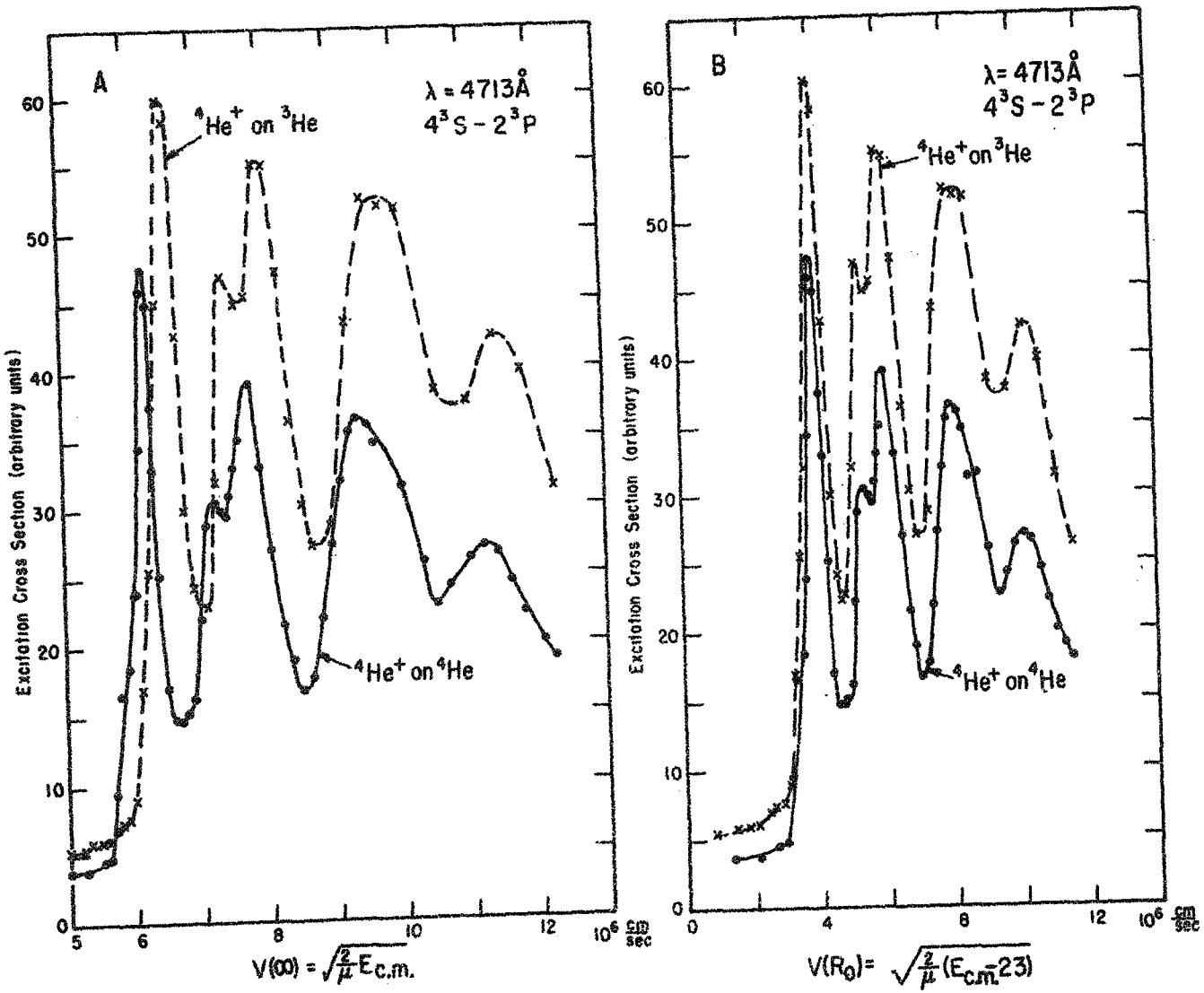

Fig. 2. (A) Excitation cross section for the 4713-Å He I line in $^4He^+ - ^4He$ and $^4He^+ - ^3He$ collisions plotted versus relative velocity at infinite internuclear separation, $v(\infty)$. (B) Excitation cross section for the 4713-Å He I line in $^4He^+ - ^4He$ and $^4He^+ - ^3He$ collisions plotted versus relative velocity in the final state.

Lifetimes and Fine Structure of the Metastable Autoionizing $(1s2s2p)\,^4P_J$ States of the Negative Helium Ion

L. M. Blau and D. Weinflash

Columbia Radiation Laboratory

and

R. Novick

Columbia Astrophysics Laboratory

Columbia University, New York, New York 10027

SUBMITTED FOR PUBLICATION
February 1970

Lifetimes and Fine Structure of the Metastable Autoionizing $(1s2s2p)\,^4P_J$ States of the Negative Helium Ion*

L. M. Blau, R. Novick, and D. Weinflash

Physics Department, Columbia University, New York, N. Y. 10027

ABSTRACT

The decay of the differentially metastable autoionizing $(1s2s2p)\,^4P_J$ states of the $^4He^-$ ion has been studied by time-of-flight techniques in an axial magnetic field, and Zeeman quenching has been observed. Two distinct lifetime components (11 μsec, 210 μsec) have been identified in a 100 eV beam with an axial field of 400 gauss. The zero-field lifetimes obtained from these and other measurements are 11 ± 5 μsec for J = 1/2, 3/2, and 345 ± 90 μsec for J = 5/2. The 5/2-3/2 fine structure interval is estimated to be 0.050 ± 0.015 cm^{-1}.

- - - - - -

The electron affinity of helium was first considered by Wu[1] in 1936 and a negatively charged state of helium was observed by Hilby[2] in 1939 using a mass spectrometer. Other experimental work[3-4] established that He^- could be produced by charge exchange collisions. Holøien and Midtal[5] employed a four-term variational wavefunction to calculate the energy of the $(1s2s2p)\,^4P_J$ states and pointed out that these states would be metastable against direct Coulomb autoionization. Although more careful computation revealed that the four-term wavefunction did not in fact lead to a positive electron affinity for the $(1s2s)\,^3S$ state, Holøien and Geltman[6]

*This work was supported by the National Aeronautics and Space Administration under grant NGR-33-008-009. It is Columbia Astrophysics Laboratory Contribution No. 19.

found that a 30-term wavefunction gave an electron affinity $E_A \geq 0.033$ eV. Brehm et al.[7] measured the electron affinity via laser photodetachment, obtaining a value $E_A = 0.080 \pm 0.002$ eV.

It was realized that the ^4P_J states could decay to the He°ground state plus a free electron by spin dependent interactions. Each J level would have a different lifetime and an external magnetic field would quench the longest-lived J = 5/2 state by mixing it with other states of the same multiplet. These predictions were experimentally verified for the corresponding ^4P_J states in Lithium.[8] Dips in the Zeeman quenching curve which result from anti-crossing levels enabled the determination of the fine-structure intervals and lifetimes for each J-state. Various authors[9-12] have calculated the lifetime of the $^4P_{5/2}$ state for atoms in the isoelectronic series, obtaining values for He^- ranging from 1700 to 266 microseconds. Since the $^4P_{5/2}$ state can decay only via the tensor spin-spin interaction, there is no ambiguity concerning the operator in the matrix element for the transition. Hence the wide range of theoretical values implies that the He^- lifetime is highly sensitive to the precise form of the wavefunctions used for the initial and final states. The theoretical lifetime increases when the initial state is described by a superposition of Hartree-Fock configurations instead of a single (1s2s2p) configuration. The electron correlation implicit in the more complicated initial wavefunction increases the average interelectron separation, thereby reducing the effectiveness of the spin-spin interaction in causing the decay. On the other hand, the theoretical lifetime decreases when the final state includes the polarization of the ($1s^2$) He° ground state by the ejected electron and the consequent distortion of the continuum wavefunction of the ejected electron by the polarized atom (see Table I). There are at

least two physical arguments that can be given for this shortening of the lifetime. First, the induced multipoles in the atom produce an attractive potential which serves to increase the density of the ejected electron in the vicinity of the atom, thereby increasing the interaction. Second, the induced multipoles themselves tend to increase the overlap of the final state of the atom with the initial state. A reliable experimental value for the lifetime is needed to evaluate the different theoretical approaches and the approximations made in the calculations.

We report herein the preliminary results of an experiment which establishes that the $J = 5/2$ lifetime is 345 ± 90 microseconds and that a weighted average of the $J = 3/2$ and $J = 1/2$ lifetimes is 11 microseconds. The 5/2 - 3/2 fine structure interval is estimated to be 0.050 ± 0.015 cm^{-1}.

In our investigation, we prepare a beam of He^- by double charge exchange, a technique proposed by Donnally.[13] A schematic representation of our apparatus is shown in Fig. 1. A 3000 eV He^+ beam is extracted from an rf discharge and passes through a potassium vapor where it suffers two collisions with neutral potassium atoms. The first collision results in a charge exchange and produces the metastable $(1s2s)\,^3S$ state of He^0. The second collision results in another charge exchange and produces the desired He^- state. The potassium vapor density can be varied to maximize the production of He^-, and negative ion currents of 100 nanoamperes are easily obtained. The beam emerging from the potassium vapor is electrostatically separated into its charge components and the total positive beam is collected as a monitor on beam stability. The He^- beam is deflected into a series of electrostatic lenses and decelerated to any desired energy above 50 eV. The beam then passes into a 10-meter drift tube solenoid-wound to provide axial magnetic fields up to 1500 gauss. The ion source and

detection regions are separated by a differential pumping aperture. The pressure on the source side is 3×10^{-6} when gas is admitted to the rf discharge, while the pressure in the detection region, which is pumped at either end by 4-in. mercury diffusion pumps, is at least an order of magnitude lower. The He^- beam is detected by a Faraday cup which is movable in the vacuum chamber nearly the full length of the drift tube. A high transparency grid, electrically insulated from the Faraday cup, is placed across the entrance of the detector. When the negative bias on the grid is greater than 20 volts, the 19.7-eV electrons produced in the beam by autoionization of He^- cannot enter the detector and the current recorded is due to He^- alone.

Figure 2 shows typical experimental results for suppression of a 150 eV He^- beam. The graphs are Faraday cup currents vs suppression voltage at successive positions of the detector. The development with increasing distance of the feature below 25 volts is evidence of the build-up of electrons in the beam, a confirmation that we are observing autoionization in flight. The sum of He^- and e^- currents at zero suppression is not independent of detector position as would be expected from conservation of charge because half the electrons are ejected backwards and hence are lost to our detector.

Data runs were taken at magnetic fields between 400 and 1500 gauss to directly observe differential metastability and Zeeman quenching. The residual pressure in the vacuum system was varied over a range from 2×10^{-7} to 3×10^{-6} Torr by regulating the water flow in the cooling lines of the solenoid. For all pressures and fields, the graph of He^- current vs distance could be fit to better than 1% by a sum of two exponentials. In Fig. 3, a run for a 100 eV H^- beam at a field of 400 gauss and a residual pressure of 2×10^{-7} Torr is fitted with lifetime components of 10.2 and 161 microseconds. The 1% accuracy of the fit to individual runs is not reflected in

a corresponding accuracy in the final result for the lifetimes because of uncontrolled changes in the residual gas pressure and beam intensity during individual runs. The closest position of the detector to the He^- source corresponds to a flight time of 7 microseconds for a 100 eV beam. If the observed relative weights of the two components are extrapolated back to the source, the weights at production are equal. The decay rate of a particular component in a given magnetic field is $\gamma_{observed} = \gamma_{natural} + n\sigma v$, where n = residual gas number density, v = beam velocity, and σ = the total cross section for removing He^- from the beam by either collisional quenching or large angle scattering. Extrapolation of $\gamma_{observed}$ to zero residual pressure was accomplished by separately varying the velocity and pressure. Figure 4 shows the dependence of the longer component, γ_L, on the product Pv. The agreement between the two methods of extrapolation is shown by the collinearity of the triangles and squares in Fig. 4. The zero-pressure decay rates of the two components at H = 400 gauss are $(4.8 \pm 0.3) \times 10^3$ sec^{-1} and $(9 \pm 1) \times 10^4$ sec^{-1}. The corresponding lifetimes are 210 and 11 microseconds. Insufficient data were obtained to make reliable pressure extrapolations for other magnetic fields. At higher fields, it was impossible to maintain a stable pressure because of the temperature rise due to Joule heating in the solenoid windings. The apparatus is being improved and better data are expected in the near future. Nevertheless, the data points in Fig. 4 for 300 gauss and 1000 gauss show an increase of the decay rate with magnetic field. Zeeman quenching was also observed by varying the magnetic field with the detector stationary at different positions. Figure 5 shows the fall off of the He^- current as a function of H^2 at three detector positions corresponding to flight times of 32, 76, and 126 microseconds.

By the hypothesis of differential-metastability, the beam should be composed of three exponential components (one for each J level) at low fields and as many as twelve components at higher fields. Our inability to resolve three distinct components deprives us of corroboration of the ^4P_J state identification. However, smoothly monotonic functions of the sort shown in Fig. 3 are notoriously difficult to fit with any uniqueness to sums of exponentials. It is completely consistent with our data that the 11 microsecond component is a weighted average of the J = 3/2 and J = 1/2 states, while the 210 microsecond component is the J = 5/2 state. The approximate equality of the weights of the two observed components lends support to this conclusion since the statistical weight of the J = 5/2 state is equal to the sum of the weights of the J = 3/2 and 1/2 states. The experimental value for the weight of the short component is 45% $\pm$ 5%. If a third very short component due to, say, the J = 1/2 state is produced and is lost in the distance the beam travels between production and detection, the relative weights of the two remaining components would be 40/60 in favor of the long component, a possibility we cannot rule out. On the other hand, the short component cannot be due to the J = 1/2 state alone because then the weights would be 25/75 in favor of the long component. We are therefore safe in assuming that the J = 3/2 lifetime, which is critical in interpreting the Zeeman quenching, is within 30% of the observed short component. Hence we will use $\gamma_{3/2} = (9 \pm 3) \times 10^4$ sec^{-1} in extrapolating γ_L to zero-field. Future plans include an effort to determine the weights more accurately and search for a third,short-lived component in a 3000-eV beam for which the flight time to the detector is reduced to 3 microseconds.

The lifetimes of the different magnetic sublevels in a magnetic field is determined by the zero-field lifetimes of the J-states and the Zeeman

mixing coefficients. At low magnetic fields where first order perturbation theory holds, J = 5/2 mixes only with J = 3/2, leading to quadratic dependence of the decay rate on H. By analogy to ^3P_J in He^o and ^4P_J in Li^o, it is expected that the 5/2 - 1/2 fine structure interval is considerably greater than the 5/2 - 3/2 interval, and hence mixing with J = 1/2 is ignored at all fields. Under the influence of a magnetic field, each M-sublevel of the J = 5/2 state goes over to a superposition of J = 5/2 and J = 3/2 with the same M:

$$|5/2,M\rangle = \cos\theta_M|5/2,M\rangle + \sin\theta_M|3/2,M\rangle \qquad (1)$$

where θ_M is a function of $\mu_o H/\Delta_{53}$ and Δ_{53} = 5/2 - 3/2 fine structure interval. The decay rate of the modified $|5/2,M\rangle$ state is given by:

$$\Gamma_M = \cos^2\theta_M\gamma_{5/2} + \sin^2\theta_M\gamma_{3/2} \qquad (2)$$

where $\gamma_{5/2}$ and $\gamma_{3/2}$ are the zero-field decay rates for J = 5/2 and J = 3/2 respectively. Because $\gamma_{3/2} >> \gamma_{5/2}$, $\Gamma_M \geq \gamma_{5/2}$, i.e., the Zeeman mixing quenches the J = 5/2 substates. At low fields, $\sin^2\theta_M$ is proportional to H^2. In particular, $\sin^2\theta_{\pm 5/2} = 0$; the $|5/2, \pm 5/2\rangle$ states remain pure at all fields. Again, because $\gamma_{3/2} >> \gamma_{5/2}$, there is a flight time $t_o \simeq 30$ microseconds beyond which essentially only J = 5/2 substates remain in the beam. The metastable current arising from the J = 5/2 substates is then:

$$I(t) = \sum_M \exp(-\Gamma_M t) \qquad (3)$$

During the flight time beyond t_o, the decay of the beam is well characterized by a single, slowly varying decay constant, γ_L. The value of γ_L at time t is equal to the logarithmic derivative of Eq. (3):

$$\gamma_L = -\frac{dI/dt}{I} = \sum_M w_M\Gamma_M / \sum w_M \qquad (4)$$

where the weights $w_M = \exp(-\Gamma_M t)$ are the relative populations of the magnetic substates after time t in the magnetic field. It is clear that γ_L first increases proportionally to H^2, and then increases less slowly, eventually saturating, and finally decreasing to its initial value $\gamma_{5/2}$ when only $|5/2, \pm 5/2\rangle$ remain in the beam. The maximum decay rate occurs at about 1000 gauss; hence γ_L at this field is not sensitive to changes in Δ_{53}. A better way to determine Δ_{53}, and from this the zero-field decay rate $\gamma_{5/2}$, is the direct observation of Zeeman quenching shown in Fig. 5. By Eq. (3), the J = 5/2 current will drop at high fields to one-third its zero-field value. This arises from complete quenching of the $M \neq \pm 5/2$ substates. With a flight time of 76 microseconds, $I - 1/3\ I_o$ drops off by a factor of e at H = 1.06 kilogauss. If $\gamma_{3/2}$ is taken to be $(9 \pm 3) \times 10^4$ sec^{-1}, then Δ_{53} must be (0.050 ± 0.015) cm^{-1} to produce the observed quenching. The zero-field decay rate inferred from $\Delta_{53} = (0.050 \pm 0.015)$ cm^{-1} and a decay rate of $(4.8 \pm 0.3) \times 10^3$ sec^{-1} at 400 gauss is $\gamma_{5/2} = (2.9 \pm 0.6) \times 10^3$ sec^{-1} or a lifetime of 345 ± 90 microseconds for J = 5/2.

These results are in apparent disagreement with the 18.2-microsecond lifetime for He^- reported by Nicholas et al.[14] However, these investigators did not consider the differential-metastability of He^- and based their conclusions on a maximum flight time of one microsecond during which they observed a 5% decay of the beam. This agrees with the decay observed during the first microsecond of our flight time when both the short and long components are present. The 345-microsecond lifetime for the J = 5/2 state is in reasonable agreement with the most recent calculation of Estberg and LaBahn[15] which takes into account distortion of the final state and yields a lifetime of 455 microseconds. In addition, our result is in agreement with an extrapolation of the $(1s2s2p)\,^4P_{5/2}$ lifetimes for the He^- isoelectronic sequence from Li^o to O^{+5}.[16] The near

degeneracy ($\Delta E = 0.050\ cm^{-1}$) of the J = 5/2 and J = 3/2 levels in He^- may be compared to the similar near degeneracy ($\Delta E = 0.070\ cm^{-1}$) of the J = 1 and J = 2 levels of the $(1s2p)\,^3P$ term of He^o. The smallness of the splitting in both cases arises from competition between the spin-spin interaction and the inverted Landé spin-orbit interaction. The small value of Δ_{53} is favorable for the scheme proposed by Feldman and Novick[17] for producing polarized ^3He nuclei by first obtaining a beam composed only of $|5/2, \pm 5/2\rangle$ and then quenching one of the M-levels by an rf resonant field.

REFERENCES

1. T. Y. Wu, Phil. Mag. 22, 837 (1936).

2. J. W. Hilby, Ann. Phys. 34, 473 (1939).

3. V. M. Dukel'skii, V.V. Asfrosimov, and N.V. Fedorenko, Sov. Phys.-JETP 3, 764 (1956).

4. P. M. Windham, P.J. Joseph, and J. A. Weinman, Phys. Rev. 109,1193 (1958).

5. E. Holøien and J. Midtdal, Proc. Phys. Soc. (London) A68, 815 (1955).

6. E. Holøien and S. Geltman, Phys. Rev. 153, 81 (1967).

7. B. Brehm, M. A. Gusinow, and J. L. Hall, Phys. Rev. Letters 19, 737 (1967).

8. P. Feldman, M. Levitt, and R. Novick, Phys. Rev. Letters 21, 331 (1968).

9. J. L. Pietenpol, Phys. Rev. Letters 7, 64 (1961).

10. C. Laughlin and A. L. Stewart, Proc. Phys. Soc. (London) (series 2,1) 151 (1968).

11. S. T. Manson, Phys. Rev. 145, 35 (1966) and private communication.

12. G. N. Estberg and R. W. LaBahn, Phys. Letters 28A, 420 (1968).

13. B. L. Donnally and George Thoeming, Phys. Rev. 159, 87 (1967).

14. J. Nicholas, C. W. Trowbridge, and W. D. Allen, Phys. Rev. 167, 38 (1968).

15. G. N. Estberg and R. W. LaBahn, Phys. Rev. Letters ___, ___ ___.

16. P. Feldman, M. Levitt, and R. Novick, Phys. Rev. Letters 21, 331 (1968).

17. P. Feldman and R. Novick, in Atomic Collision Processes, McDowell, ed., Proc. Third International Conf. on the Physics of Electronic and Atomic Collisions [North Holland Publishing Co., Amsterdam (1964) p. 201].

FIGURE CAPTIONS

Fig. 1. Schematic diagram of the He^- source and detection regions.

Fig. 2. Current reaching the movable Faraday cup at successive detector positions as a function of negative suppression voltage. Note the buildup of the low energy component and the decrease of the high energy component as the detector is moved away from the source.

Fig. 3. Typical He^- data run fitted to a sum of two exponentials. The two components have equal weight when extrapolated back to the source, which is located at D = -1.2 meters.

Fig. 4. The decay constant of the long-lived He^- component, γ_L, as a function of pressure times velocity at several magnetic fields.

Fig. 5. Quenchable component of the He^- current as a function of H^2 with the detector stationary at positions corresponding to flight times of 32, 75, and 126 microseconds. At these flight times, the metastable current is due essentially only to the J = 5/2 substates. One third of the zero-field J = 5/2 current arises from $M_J = \pm 5/2$, which is not quenched by Zeeman mixing and is therefore subtracted from the total current.

Table I. Theoretical values for the lifetime of the $(1s2s2p)\,^4P_{5/2}$ state of He^- (in μsec).

		No. of configurations in initial state wavefunction	
		N = 1	N = 28
Polarization of the final state included	no	303[a]	550[a]
	yes	266[b]	455[c]
Present experimental value		345 ± 90[d]	

[a]Ref. 10, [b]Ref. 12, [c]Ref. 15, [d]present work.

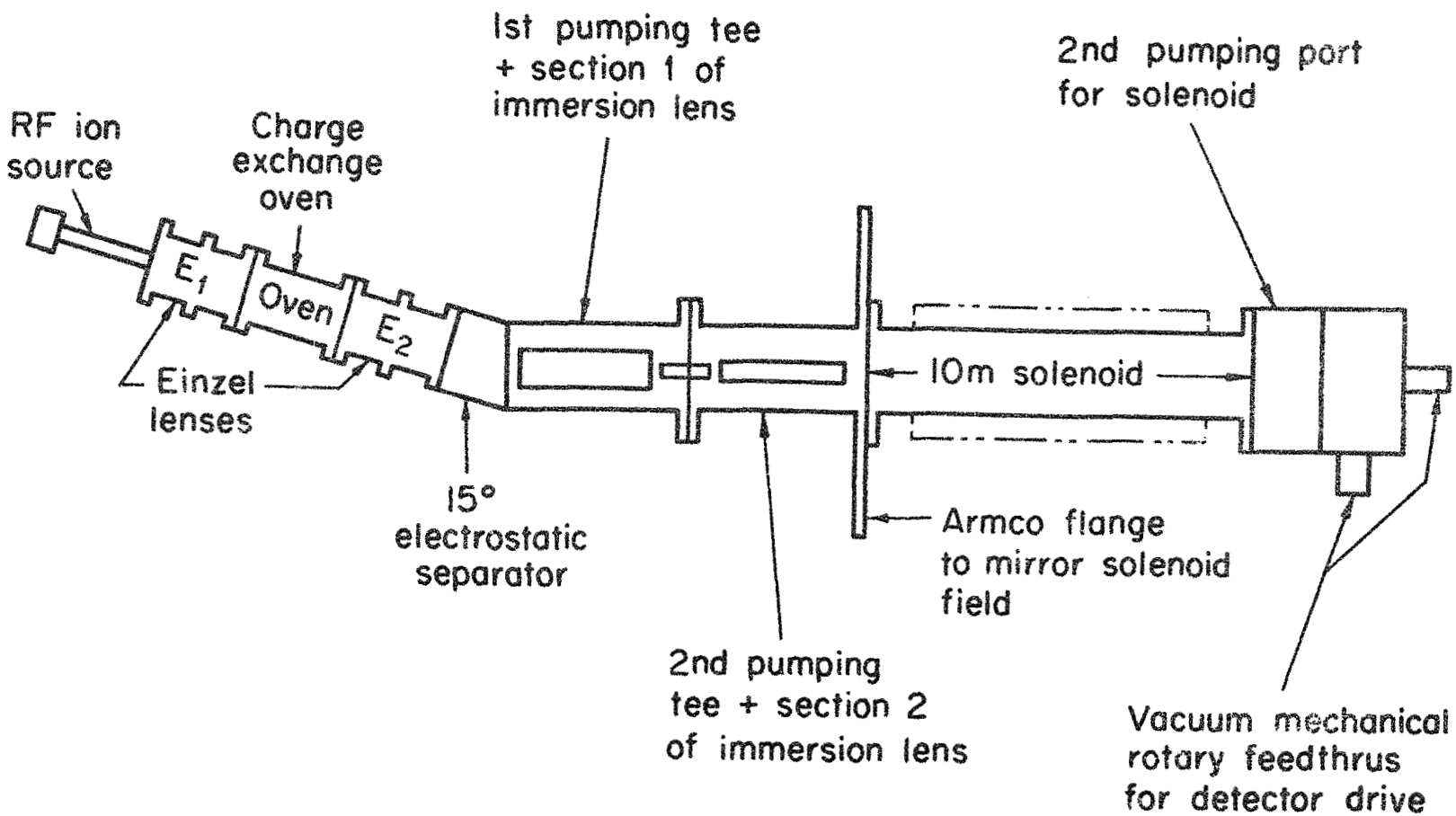

Fig. 1. Schematic diagram of the He^- source and detection regions.

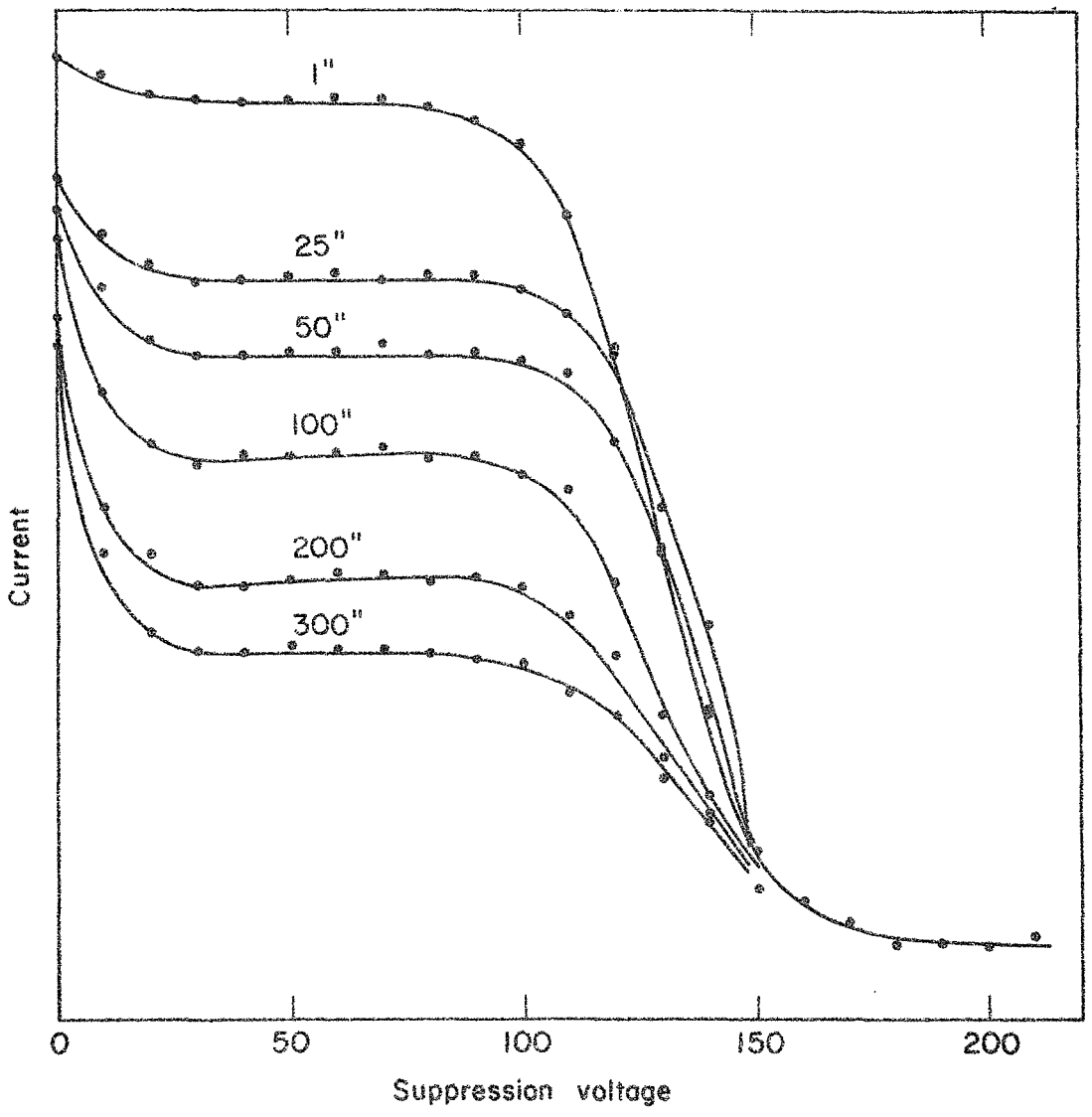

Fig. 2. Current reaching the movable Faraday cup at successive detector positions as a function of negative suppression voltage. Note the buildup of the low energy component and the decrease of the high energy component as the detector is moved away from the source.

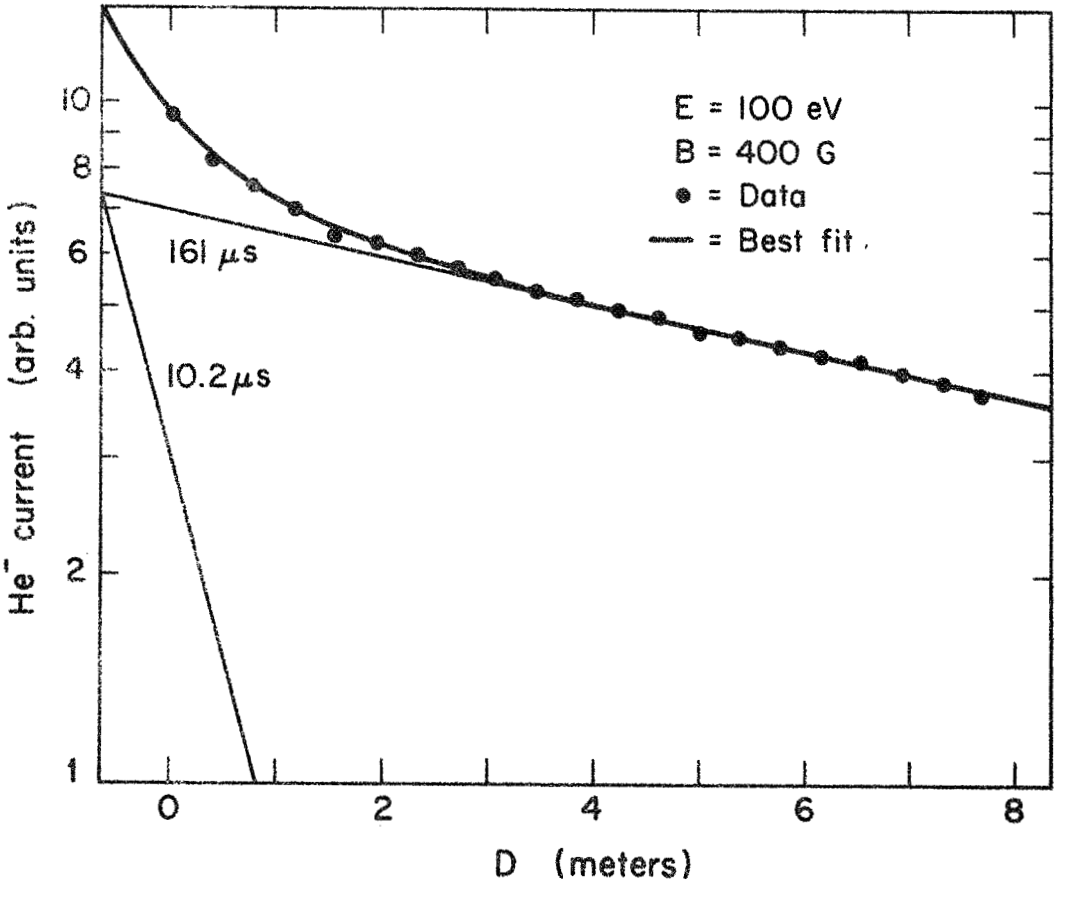

Fig. 3. Typical He^- data run fitted to a sum of two exponentials. The two components have equal weight when extrapolated back to the source, which is located at D = -1.2 meters.

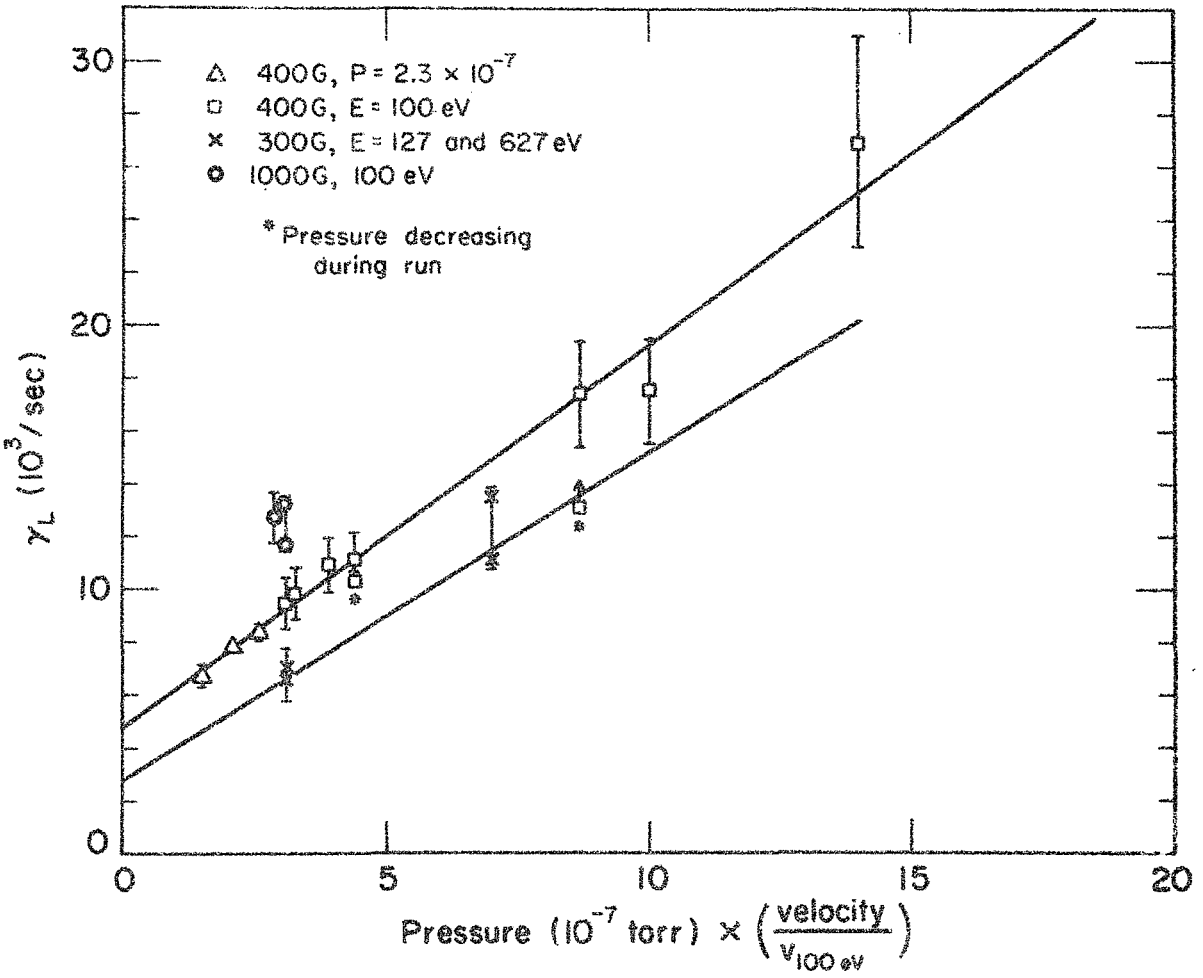

Fig. 4. The decay constant of the long-lived He^- component, γ_L, as a function of pressure times velocity at several magnetic fields.

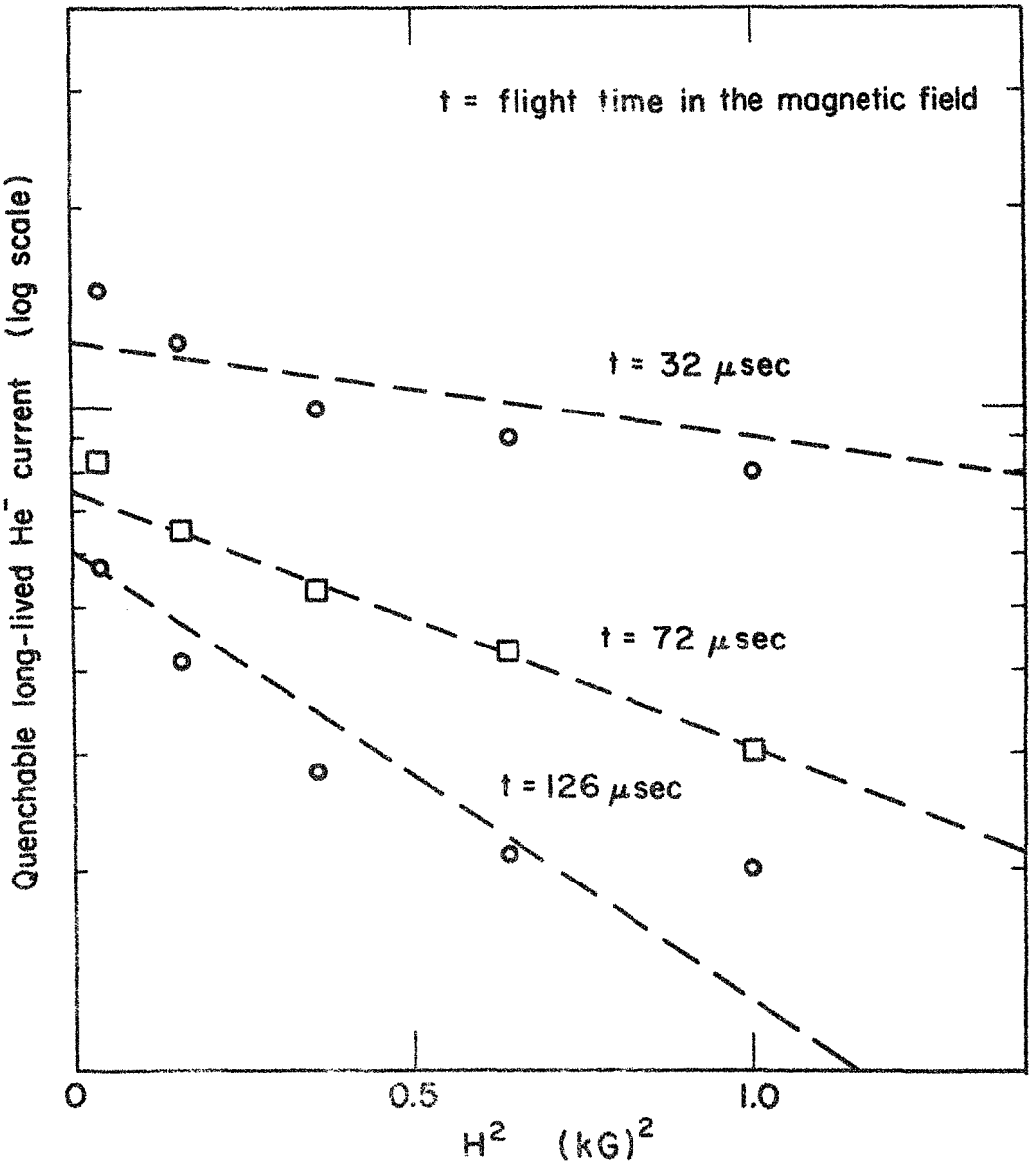

Fig. 5. Quenchable component of the He^- current as a function of H^2 with the detector stationary at positions corresponding to flight times of 32, 72, and 126 microseconds. At these flight times, the metastable current is due essentially only to the J = 5/2 substates. One third of the zero-field J = 5/2 current arises from $M_J = \pm 5/2$, which is not quenched by Zeeman mixing and is therefore subtracted from the total current.

PRECISION MEASUREMENT OF THE FINE STRUCTURE AND LIFETIMES OF THE $(1s2s2p)\,^4P_J$ STATES OF He^- AND Li*

Robert Novick and David Weinflash

Department of Physics
Columbia University
New York, New York 10027

For Proceedings of the International Conference

on Precision Measurements and Fundamental Constants

National Bureau of Standards
Gaithersburg, Maryland

August 3 - 7, 1970

PRECISION MEASUREMENT OF THE FINE STRUCTURE AND LIFETIMES OF THE $(1s2s2p)^4P_J$ STATES OF He^- AND Li*

Robert Novick† and David Weinflash

Department of Physics, Columbia University

Abstract

A series of measurements has been completed and others are in progress for the precise determination of the energies and lifetimes of the metastable autoionizing $(1s2s2p)^4P_J$ states in He^- and Li*. Since these states have lifetimes in the range from 5 to 500 μsec and since the fine and hyperfine structure intervals are of the order of a wave number, it will be possible to determine the splitting with a relative accuracy of one part in 10^6 or better. Present measurements in Li^6 and Li^7 are at the level of one part in 10^4 and a preliminary crude estimate has been made of the $^4P_{5/2}-^4P_{3/2}$ interval in He^-. Further work is in progress with radio-frequency techniques to obtain very much more precise results. Considerable theoretical effort must be made before these results can be interpreted in terms of fundamental constants. However, it is clear that if the necessary numerical wavefunctions can be obtained with sufficient accuracy, and if the various radiative and relativistic corrections can be evaluated, then these results will provide a precise new independent value for the Sommerfeld fine structure constant.

† Work supported by National Aeronautics and Space Administration under Grant NSG-360 and by National Science Foundation, Grant NSFGP-13749.

1. Introduction

The metastable autoionizing $(1s2s2p)\,^4P_J$ states of He^- and Li^* provide an unusual opportunity to check the accuracy of quantum calculations for three-electron systems. The fine-structure intervals and lifetimes of these states are a sensitive test of our understanding of electron correlation effects and the competition between various spin-dependent interactions. In addition, the Fermi contact hyperfine interaction of the unpaired s-electrons provides a critical test of our ability to calculate the electron density at the nucleus. If numerical wavefunctions are obtained with sufficient accuracy and the various radiative and relativistic corrections are evaluated, very precise measurements of the level splittings will provide an independent value for the Sommerfeld fine-structure constant, α, accurate to six places or better. Alternatively, if we assume that α is known from other work, then such precise experimental values could be used either as a new test of quantum electrodynamics or to place limits on new interaction terms that may be postulated for the Hamiltonian of simple atomic systems [1].

The feature of these states which lends them to high precision measurement is their metastability: they are stable against electric-dipole emission and decay only by spin-dependent autoionization to a ground state configuration plus a free electron. The lifetimes are in the range from 5 to 500 μsec, implying natural widths as low as 2 kHz. The resolution of an rf resonance will be limited only by field homogeneity and the time spent in the rf region, which may be as long as 100 μsec. Since the levels are separated by $\sim 1\ cm^{-1}$, it will be possible to determine the levels with a relative accuracy of one part in 10^6 or better.

A further important property of these states is that each level of the ^4P_J multiplet has a different lifetime. Hence, differential populations are spontaneously created in flight, both between J-levels, and in an axial static magnetic field, between M_J-levels (Zeeman quenching). This effect can be exploited for state selection and the production of polarized particles.

2. Metastable Autoionizing States

The earliest interest in atomic states metastable against both autoionization and radiative decay concerned attempts to understand the existence of the helium negative ion, first observed by Hilby [2]. The possibility of this ion existing in the lithium-like $(1s^2 2s)^2S_{1/2}$ ground state configuration was rejected when variational calculations [3] failed to show a positive electron affinity.[1]

G. J. Schulz has reported the observation of a resonance in the elastic scattering of electrons on helium at 0.46 eV which he attributes to the formation of a temporary negative ion with the configuration $(1s^2 2s)$. See Proceedings of the Fourth International Conference on the Physics of Electronic and Atomic Collisions, Quebec, 1965, edited by L. Kerwin and W. Fite (Science Bookcrafters, Inc., Hastings-on-Hudson, New York, 1965), p. 117.

Ta-You Wu suggested [4] that the $(1s2s2p)^4P$ term of He^-, in which two of the electrons are excited, could be bound with respect to the $(1s2s)^3S$ term of neutral helium. Elaborate variational calculations have confirmed this conjecture, but at least 20 terms are required in the wavefunction to produce a positive electron affinity for helium in the $(1s2s)^3S$ state [5]. The selection rule $\Delta S = 0$ forbids decay to the helium ground state plus a free electron by either electric-dipole emission or by autoionization via the Coulomb potential between the electrons. The state is therefore metastable and was postulated to account for the observations of He^-.

Analogous metastable autoionizing states were predicted for the alkalis. These quartet states are produced by the excitation of a single core electron and have energies much greater than the first ionization potential of the atom. Of particular interest in the present connection are the $(1s2s2p)^4P_J$ states of lithium which have exactly the same configuration as predicted for He^-. The $\Delta S = 0$ selection rule makes Li^*, like He^-, metastable with a lifetime of a few μsec.

It was realized [6] that the breakdown of LS coupling in both He^- and Li^* would mix all but the $^4P_{5/2}$ state with ^2P states which autoionized very rapidly (lifetime on the order of one Bohr period: $\sim 10^{-14}$ sec). Thus even a very small doublet admixture would strongly quench the $^4P_{3/2}$ and $^4P_{1/2}$ states. Finally, Kroll pointed out that even $^4P_{5/2}$ could decay by the tensor part of the spin-spin interaction. The $^4P_{3/2}$ and $^4P_{1/2}$ states can also decay directly by spin-dependent interactions as well as indirectly via the doublets, leading to generally shorter lifetimes. In the case of Li^*, the metastable state has an energy of 57 eV, or more than ten times the first ionization energy of Li, yet its lifetime is about 6 μsec.

The term "differential metastability" has been coined to describe the existence of distinct lifetimes for each J-state of the multiplet. A further proliferation of lifetimes occurs in an external magnetic field and/or in the presence of hyperfine structure.

In the exploratory work carried out so far, the splittings of the $^4P_{J,F}$ states are obtained by diagonalizing a semi-phenomenological Hamiltonian which includes fine and hyperfine structure terms as well as the Zeeman interaction:

$$H = c_{SO}\vec{L}\cdot\vec{S} + c_{SS}\,[3(\vec{L}\cdot\vec{S})^2 + 3/2(\vec{L}\cdot\vec{S}) - L(L+1)S(S+1)] + a_c\vec{I}\cdot\vec{S} + \mu_o H(g_L L_z + g_S L_z + g_I I_z)\ . \quad (1)$$

Magnetic dipole and electric quadrupole hyperfine terms were also included in the analysis, but were not varied in fitting data [7]. In the absence of hyperfine structure, let the eigenstates of given M_J in an external magnetic field be indexed by the superscript i:

$$|\psi^i_M(H)\rangle = \Sigma_J\ a^i_{JM}(H)\,|J,M\rangle\ . \quad (2)$$

If the separation between the levels is large compared to their width, the decay rate of $|\psi^i_M(H)\rangle$ is well-defined and given by a weighted sum of the zero-field decay rates γ_J of the multiplet:

$$\gamma^i_M(H) = \Sigma_J\ |a^i_{JM}(H)|^2\gamma_J\ . \quad (3)$$

Expressions of the same form as eqs. (2) and (3), with M replaced by F, give the eigenstates and decay rates of the hyperfine levels with no external field. The state of highest F ($F_{max} = 5/2 + I$) is a pure $J = 5/2$ state and thus in general is longest-lived. With both hyperfine and external fields, the summation in eq. (3) extends over J and F to obtain the decay rates for states with a given M_F. The most important conse-

quence of the mixing by an external field is to increase the decay rate of the $^4P_{5/2,F}$ states, thereby "Zeeman quenching" the metastable signal reaching the detector in an atomic beam experiment. However, the state of highest F and $|M_F|$ is not mixed and retains the pure $^4P_{5/2}$ decay rate, $\gamma_{5/2}$.

3. Lithium

The early work on lithium and the other alkalis established the existence of autoionizing states with lifetimes in the μsec range [8]. A schematic diagram of the apparatus used in these investigations is shown in figure 1. A beam of metastable atoms was produced by electron bombardment of lithium atoms emanating from an oven. The metastables were detected by collecting the ion-electron pairs that result from autoionization. The original detector was simply a pair of parallel metal plates with a small potential across them to enhance collection efficiency. Greater sensitivity was achieved by replacing the metal plates with a magnetic strip electron multiplier. To prevent charged particles from entering the detector, a honeycomb grid was placed across the entrance. The threshold in lithium for the excitation of the metastable signal was 57.3 ± 0.3 volts. Since the creation of the metastable involves a spin flip, the excitation function is characteristic of exchange collisions: the cross section attains its maximum within a few eV of the threshold energy and then decreases very rapidly. An auxiliary detector downstream from the main detector was sensitive to photons and metastables but not the ion-electron pairs, and showed no marked increase in signal strength at the metastable threshold.

The metastable detector was movable over a distance of 3 cm and the lifetime of the lithium metastable, which was assumed to be pure $^4P_{5/2}$ by the time it reached the detector, was determined to be 5.1 ± 1.0 μsec.

Quenching of the metastable signal by electric and magnetic fields was also observed. The magnetic quenching curves of Li^7 and Li^6 showed several resonance-like dips which were attributed to strong mixing of short-lived and long-lived states at level anticrossings. The quenching curves for both isotopes were studied in greater detail with the entire apparatus (source and detector) enclosed in a uniform magnetic field to prevent non-adiabatic transitions in the fringing region [7]. Typical data for Li^7 are reproduced in figure 2. Three anticrossing dips in Li^7 were investigated and ascribed to long-lived $J \approx 5/2$ levels anticrossing short-lived $J \approx 1/2$ levels. The anticrossing levels are illustrated in figure 3. In Li^6, three anticrossings of $J \approx 5/2$ states were found: two involving $J \approx 3/2$ states and one involving a $J \approx 1/2$ state. The centers of the dips were accurately located, and the widths measured, by signal-averaging techniques.

A theoretical analysis showed that in the vicinity of the anti-crossings, a two-state treatment of the levels is adequate. The fine-structure intervals $^4P_{5/2}-^4P_{3/2}$ ($\equiv \Delta_{53}$) and $^4P_{5/2}-^4P_{1/2}$ ($\equiv \Delta_{51}$) were determined to a few parts in 10^4 by finding, and demonstrating the uniqueness of, a set of values for a_{SO}, a_{SS}, and a_c in eq. (1) that gave anticrossings in Li^6 and Li^7 at the experimentally observed fields. The $^4P_{5/2}$ and $^4P_{1/2}$ lifetimes were determined by the widths of the corresponding anticrossings. Finally, the $^4P_{5/2}$ lifetime was re-evaluated, taking into account the considerable hyperfine mixing, which raised the value about 16% [9]. The results for the energies of the $(1s2s2p)\,^4P_{J,F}$ states of Li^7 appear in figure 4. The lifetimes and structure constants are given in table 1.

This work provided the first definitive assignments for lines observed in the course of a study of the LiII spectrum [10] which had no place in the normal spectra of the atom or ion. It had been suggested that these lines arose from transitions to the metastable $(1s2s2p)^4P_{J,F}$ ground quartet-state from higher quartets. Assuming the upper state to be $(1s2s3s)^4S$, the new experimental results for the level structure of $(1s2s2p)^4P_{J,F}$ in Li^7 were used to calculate a theoretical line shape for the unassigned 2934 Å line. The calculated line profile is in excellent agreement with the spectroscopic data [7]. This agreement strongly supports the term assignments and the structure of the ^4P_J states.

The level scheme described above predicts the location of <u>crossings</u> between states of different M_F to within one gauss. These states can be coupled in the neighborhood of the crossings by an appropriate rf magnetic field oscillating perpendicular to the static field H_o, and transitions detected by a drop in metastable signal. Under favorable experimental circumstances, the line width is determined only by the natural width of the short-lived state, which is ~0.25 MHz for $J \approx 3/2$ and ~0.75 MHz for $J \approx 1/2$. Determination of the fine and hyperfine structure could be about 200 times more accurate than in the static quenching experiment and precision of a few parts in 10^6 or better could be achieved. Tentative identification of a 30 MHz resonance in Li^7 at 5374 gauss has been made [11]. This is roughly 3 gauss below the crossing of a $J \approx 3/2$, $F = 1$, $M_F = 0$ level with a $J \approx 5/2$, $F = 1$, $M_F = -1$ level, as calculated from the level scheme of figure 4. The resonance has proved to be elusive and work is continuing on this and other predicted hyperfine resonances.

4. The Helium Negative Ion

Results on the helium negative ion, which prompted the whole line of research, are as yet primitive, at least for the fine-structure. The negative ion of the He^4 isotope (I=0) has been studied by time-of-flight techniques in an axial magnetic field and Zeeman quenching observed at fields as low as 400 gauss. Lifetimes of roughly 500, 10, and 16 μsec have been obtained for the J = 5/2, 3/2 and 1/2 states respectively.[2] In addition, the $^4P_{5/2}$-$^4P_{3/2}$ fine-structure interval has been estimated to be 0.036 ± 0.009 cm^{-1} from the Zeeman quenching data between 350 and 1400 gauss [12].

[2] These lifetimes are in apparent disagreement with an 18.2 μsec lifetime for He^- reported by Nicholas, Trowbridge, and Allen, Phys. Rev. 167, 38 (1968). However, these investigators did not consider the differential metastability of He^- and based their conclusions on a maximum flight time of 1 μsec during which they observed a ~5% decay of their beam. This agrees with the decay observed during the first microsecond of decay in our work when both the long-lived and short-lived components are present in the beam.

Figure 5 is a schematic diagram of the apparatus used in the study of He^-. A beam of the negative ion is prepared by double charge exchange, a technique proposed by Donnally [13]. A 3000-eV He^+ beam is extracted from a 80 MHz rf discharge and passes through a potassium vapor where it suffers two collisions with neutral potassium atoms. The first collision produces the metastable $(1s2s)^3S$ state of He^o. The second collision results in another charge exchange and produces the desired He^- state. The potassium vapor density can be varied to maximize the production of He^- and a negative ion current of 100 nA is easily obtained. The beam emerging from the potassium vapor is electrostatically separated into its charge components and the total positive beam is collected as a monitor on beam stability. The He^- beam is deflected into a series of electrostatic lenses and decelerated to any desired energy above ~50 eV. The beam then passes into a 10-meter drift tube wound to provide axial magnetic fields up to 1500 gauss. The ion source and detection regions are separated by a differential-pumping aperture. The pressure on the source side is 3×10^{-6} Torr when helium gas is admitted to the rf discharge, while the pressure in the detection region is at least an order of magnitude lower.

The He^- beam is detected by a Faraday cup which is movable in vacuum nearly the full length of the drift tube. A high transparency grid, electrically insulated from the Faraday cup, is placed across the entrance of the detector. When the negative retarding voltage on the grid is greater than 20 volts, the 19.7-eV electrons produced by autoionization in flight of He^- cannot enter the detector and the current recorded is due to He^- alone.

The dependence of the He^- metastable beam intensity on the experimental variables (distance from source, magnetic field, beam velocity, and residual gas pressure) was analyzed to extract the lifetimes and fine-structure of the $(1s2s2p)\,^4P_J$ states of He^-. The bulk of the data was taken at a beam energy of 100 eV and a field of 400 gauss. The plot of metastable current versus distance is fit in all cases to 1% by a weighted sum of two exponential components. The closest position of the detector to the source corresponds to a flight time of 7 μsec for a 100-eV beam. If the observed weights are extrapolated back to the source, the intensities at production are roughly equal. The decay rate γ_S of the short-lived component was essentially independent of field, velocity, and pressure. The decay rate γ_L of the long-lived component increased with all these variables, and was extrapolated to zero residual pressure using data at various pressures and velocities. The long-lived component was identified with a weighted average of the $^4P_{5/2}$ substates, while the short-lived component was assumed to be an average of the $^4P_{3/2}$ and $^4P_{1/2}$ states. This assignment is supported by the agreement between the relative strengths of the two components with their statistical weights and the increase of the decay rate of the long-lived component with magnetic field.

More detailed information on the lifetimes and fine-structure intervals was obtained directly from the Zeeman quenching curves. The field dependence of the metastable current (shown in figure 6) yielded values for the $^4P_{5/2}$-$^4P_{3/2}$ fine-structure interval Δ_{53} and the difference between the $^4P_{3/2}$ and $^4P_{5/2}$ decay rates, $\gamma_{3/2}$-$\gamma_{5/2}$. With these two atomic parameters fixed, all three zero-field decay rates were determined from the decay-length data. In figure 7, the data is fit with three exponential components. The weights extrapolated back to the source at S are

proportional to the statistical weights of the assigned J-values. Only the $^4P_{5/2}$-$^4P_{1/2}$ fine-structure interval, Δ_{51}, remains inaccessible to the present experimental approach. Table 2 gives the preliminary lifetimes and fine-structure obtained in this work.

There are probably no narrow anticrossings in the negative ion of the isotope He^3 (I=1/2) such as those observed in Li^6 and Li^7. Manson's [14] theoretical level diagram for the He^3 ion is shown in figure 8. The hyperfine splitting is calculated to be considerably larger than the Δ_{53} fine-structure interval and comparable to the Δ_{51} interval. Narrow anticrossings occur between states which would in fact cross if they were not weakly coupled by a perturbation small compared to the Hamiltonian which defines them. There are broad Zeeman anticrossings in the energy levels for ions of both He isotopes, but these are of little experimental interest and despite the smallness of Δ_{53}, the lowest of these occurs around 3700 gauss, still too high for the present apparatus. It would be prohibitive to produce a magnetic field more than a few kilogauss over a distance sufficient to appreciably quench the long-lived He^- states. These states mix with "short-lived" states that have lifetimes ~10 μsec, or decay lengths of ~70 cm for a 100-eV beam.

Although not expected to exhibit anticrossings, the Zeeman quenching curve of the He^3 ion could give a value for Δ_{51}, the atomic parameter unmeasured by the work to date. Denote as F = 1' and F = 2' the hyperfine states with $J \approx 3/2$ to distinguish them from the states F = 1, $J \approx 1/2$ and F = 2, $J \approx 5/2$. Because $\Delta_{53} < 0$, we would expect $\Delta_{32'} < 0$ and $\Delta_{21'} < 0$ in figure 8. However, Manson's calculation gives $\Delta_{21'} > 0$; i.e., F = 2 is higher then F = 1' because the latter is depressed by repulsion from F = 1. This depression of the F = 1' level is sensitive to the value of Δ_{51}. It is possible that Δ_{51} is actually too large to

cause inversion of F = 1' and F = 2, as Manson claims. If $\Delta_{21'}$ is significantly different from $\Delta_{32'}$, very precise Zeeman quenching data for the He^3 ion could determine the absolute value of $\Delta_{21'}$, although unfortunately not its sign. If the actual splittings are favorable, a value for Δ_{51} could be obtained by this method.

Very sharp rf resonances could be obtained at low frequency in the neighborhood of level crossings in the ion of either isotope. There are four $\Delta M_J = -1$ crossings in the He^3 ion between 400 and 700 gauss suitable for low-frequency π-transitions. They occur where $|J=5/2,M+1\rangle$ intersects $|J=3/2,M\rangle$, for $-3/2 \leq M \leq +3/2$. The location of the crossing with $M_{3/2} = +3/2$ depends only on Δ_{53}; the location of the crossing with $M_{3/2} = -3/2$ is influenced strongly by Δ_{51}. Similar crossings occur in the He^3 ion between F = 3 and F = 2' and between F = 2 and F = 1'. The contributions to the line width are: (1) rf power level, which can be made low once the resonance is located; (2) time spent by the ion in the rf field, which can be as long as 100 μsec; (3) inhomogeneities in the static magnetic field; (4) natural decay width of the short-lived state, which is ~100 KHz.

At such time as resonance techniques are successfully applied to this problem there will be a number of radio frequency and microwave transitions that can be readily studied. If we conservatively estimate that the line center can be determined to 1/10 of its width, we can measure the intervals in He^- and Li^* to one part in 10^6 or better. This is an order of magnitude more precise than results for systems that are not metastable. For example, the 2^3P_1-2^3P_2 fine-structure interval in the $(1s2p)^3P_J$ state of neutral helium was measured by optical level crossing to 40 ppm [15]. The line-width of 2.7 gauss, equivalent to several MHz, arose from the radiative lifetime (~10^{-7} sec) of the allowed-electric-dipole transition to $(1s2s)^3S$. A more recent determination of

this interval by an atomic-beam optical-microwave resonance method is accurate to 3 ppm [16]. However, this precision is based on fitting the data to a theoretical line shape and locating the center of the line to 1.2×10^{-3} of its width. In hydrogen, the linewidth of the 2^2P state is about 100 MHz, or roughly 1% of the $^2P_{3/2}$-$^2P_{1/2}$ fine-structure separation.

5. Comparison to Theoretical Work

As might be expected, the agreement between theory and experiment is better for Li^* than for the weakly-bound He^-. Several calculations of the $(1s2s2p)^4P$ term energy in lithium are within the experimental limits of 57.3 ± 0.3 eV above the $(1s^2 2s)$ ground state (see Table II of ref. 8). Manson's values in lithium for the $^4P_{5/2}$ lifetime [17], the spin-spin constant c_{SS}, and the hyperfine constant a_c [14] are all in good agreement with experiment. The only serious discrepancy is in the value of the spin-orbit constant c_{SO}; the theoretical value is roughly twice the experimental value. In the $(1s2s2p)^4P_J$ states, c_{SO} includes a negative contribution from the magnetic field produced by the p-electron on the unpaired spins of the s-electrons, called the spin-other-orbit interaction. This overpowers the usual spin-orbit energy due to the p-electron orbit producing a magnetic field on its own spin; the net orbital interaction makes c_{SO} negative. Because c_{SO} is the difference of two comparable quantities, it is very sensitive to electron correlation effects, the exact form of the wavefunction, etc.

The situation is more difficult for He^-. The largest electron affinity obtained for He by variational calculations is Weiss' value of 0.069 eV [4], which is about 14% smaller than the experimental value of 0.080 ± 0.002 eV measured via a laser photo-detachment technique by

Brehm, Gusinow, and Hall [18]. Since the energy is the quantity most accurately calculated by variational techniques, the other quantities evaluated using these wavefunctions are in serious doubt.

The preliminary experimental value for the Δ_{53} fine-structure splitting is about half the theoretical splitting. If the theoretical value for c_{SS} is assumed to be accurate, as is suggested by the agreement in Li^*, the experimental value for Δ_{53} can be used to estimate values for c_{SO} and Δ_{51} (see table 2).

Theoretical values for the lifetime of $^4P_{5/2}$ in He^- ranging from 266 to 1700 μsec can be found in the literature [19, 20]. Most recent calculations include electron correlation in the initial state through a multi-term variational wavefunction. The most sophisticated calculation considers the effects of polarization of the $(1s^2)$ final state by the free electron and the consequent distortion of the continuum wavefunction [21]. Because the $^4P_{5/2}$ state can decay only via the tensor part of the spin-spin interaction, there is no ambiguity concerning the operator in the matrix element of the transition. A reliable and precise experimental value for the lifetime is therefore a clearcut test of the initial and final state wavefunctions and should inspire further theoretical efforts.

Future experimental efforts will aim at finding and precisely measuring the rf and microwave resonances described above. If the anticipated precision is obtained, the results will provide rigorous constraints on theoretical discussions of the three-electron system. Theoretical groups are considering the possibility of calculating very precise numerical non-relativistic wavefunctions for three-electron states [22]. Clearly such results will be essential to the interpretation of the high precision experimental studies.

Table 1

Fine-Structure and Lifetime of $(1s2s2p)\,^4P_J$ in Li*

(intervals in mK = 10^{-3} cm^{-1}; lifetimes in μsec)

quantity	experiment[a]	theory[b]
Δ_{53} ($^4P_{5/2}$-$^4P_{3/2}$)	+997.34 ± 0.66	+ 575
Δ_{51} ($^4P_{5/2}$-$^4P_{1/2}$)	-1724.70 ± 0.54	-2610
c_{SO}	-154.47 ± 0.30	- 325
c_{SS}	+184.47 ± 0.14	+ 185
$a_c(Li^7)$	+172.09 ± 1.12	+ 172
$a_c(Li^6)$	+ 65.16 ± 0.42	+ 65
$\tau_{5/2}$	5.8 ± 1.2	5.88
$\tau_{3/2}$	0.46 ± 0.10	0.30
$\tau_{1/2}$	0.14 ± 0.07	>10.0*

* Involved large cancelation due to interference

(a) References 7, 9

(b) Reference 14

Table 2

Fine-Structure and Lifetimes of $(1s2s2p)\,^4P_J$ in $^4He^-$

(intervals in mK = 10^{-3} cm^{-1}; lifetimes in μsec)

quantity	experimental[a]	theory[b]
Δ_{53} ($^4P_{5/2}$-$^4P_{3/2}$)	± 36 ± 9	-68
Δ_{51} ($^4P_{5/2}$-$^4P_{3/2}$)	-263*	-314
c_{SO}	-49	-61.3
c_{SS}	11.4	11.4
a_c	---	-101
$\tau_{5/2}$	500 ± 200†	1000
$\tau_{3/2}$	10 ± 2	33
$\tau_{1/2}$	16 ± 4	3500§

* There is only experimental data for $|\Delta_{53}|$; the rest of experimental column uses Δ_{53} = -36 and theoretical c_{SS} to calculate Δ_{51} and c_{SO}.

† See footnote 2.

§ Involved large cancelation due to interference.

(a) Reference 12

(b) Reference 14

References

[1] B. Sakitt and G. Feinberg, Phys. Rev. 151, 1341 (1966).

[2] J. W. Hilby, Ann. Physik 34, 473 (1939).

[3] Ta-You Wu, Phil Mag. 22, 837 (1936).

[4] Ta-You Wu, Phys. Rev. 58, 1114 (1940).

[5] E. Holøien and S. Geltman, Phys. Rev. 153, 81 (1967). This reference contains previously unpublished work of A. W. Weiss.

[6] E. Holøien and J. Midtdal, Proc. Phys. Soc. (London) A68, 815 (1955); 90, 883 (1967).

[7] P. Feldman, M. Levitt, and R. Novick, Phys. Rev. Letters 21, 331 (1968).

[8] P. Feldman and R. Novick, Phys. Rev. Letters 11, 278 (1963); "Atomic Collision Processes," edited by M. R. C. McDowell (North-Holland Publishing Company, Amsterdam, 1964), pp. 201-210; Phys. Rev. 160, 143 (1967).

[9] P. Feldman, M. Levitt, and R. Novick, Phys. Rev. (to be published).

[10] G. Herzberg and H. R. Moore, Can J. Phys. 37, 1293 (1959).

[11] M. Levitt, R. Novick, and S. Skwire, "Columbia Radiation Laboratory Progress Report No. 19" (1969), page 6.

[12] L. M. Blau, R. Novick, and D. Weinflash, Phys. Rev. Letters 24, 1268 (1970). New data has been obtained on He^- and the data in this paper re-analyzed.

[13] B. L. Donnally and G. Thoeming, Phys. Rev. 159, 87 (1967).

[14] S. T. Manson, Phys. Rev. (to be published).

[15] F. D. Colegrove, P. A. Franken, R. R. Lewis, and R. H. Sands, Phys. Rev. Letters 3, 420 (1959).

[16] F. M. J. Pichanick, R. D. Swift, C. E. Johnson, and V. W. Hughes, Phys. Rev. 169, 55 (1968).

[17] S. T. Manson, Phys. Rev. 145, 35 (1966); Phys. Rev. Letters 23, 315 (1966).

[18] B. Brehm, M. A. Gusinow, and J. L. Hall, Phys. Rev. Letters 19, 737 (1967).

[19] J. L. Pietenpol, Phys. Rev. Letters 7, 64 (1961).

[20] C. Laughlin and A. L. Stewart, J. Phys. B: Proc. Phys. Soc. (London) 1, 151 (1968).

[21] G. N. Estberg and R. W. LaBahn, Phys. Letters 28A, 420 (1968); Phys. Rev. Letters 24, 1265 (1970).

[22] Verne Jacobs (private communication).

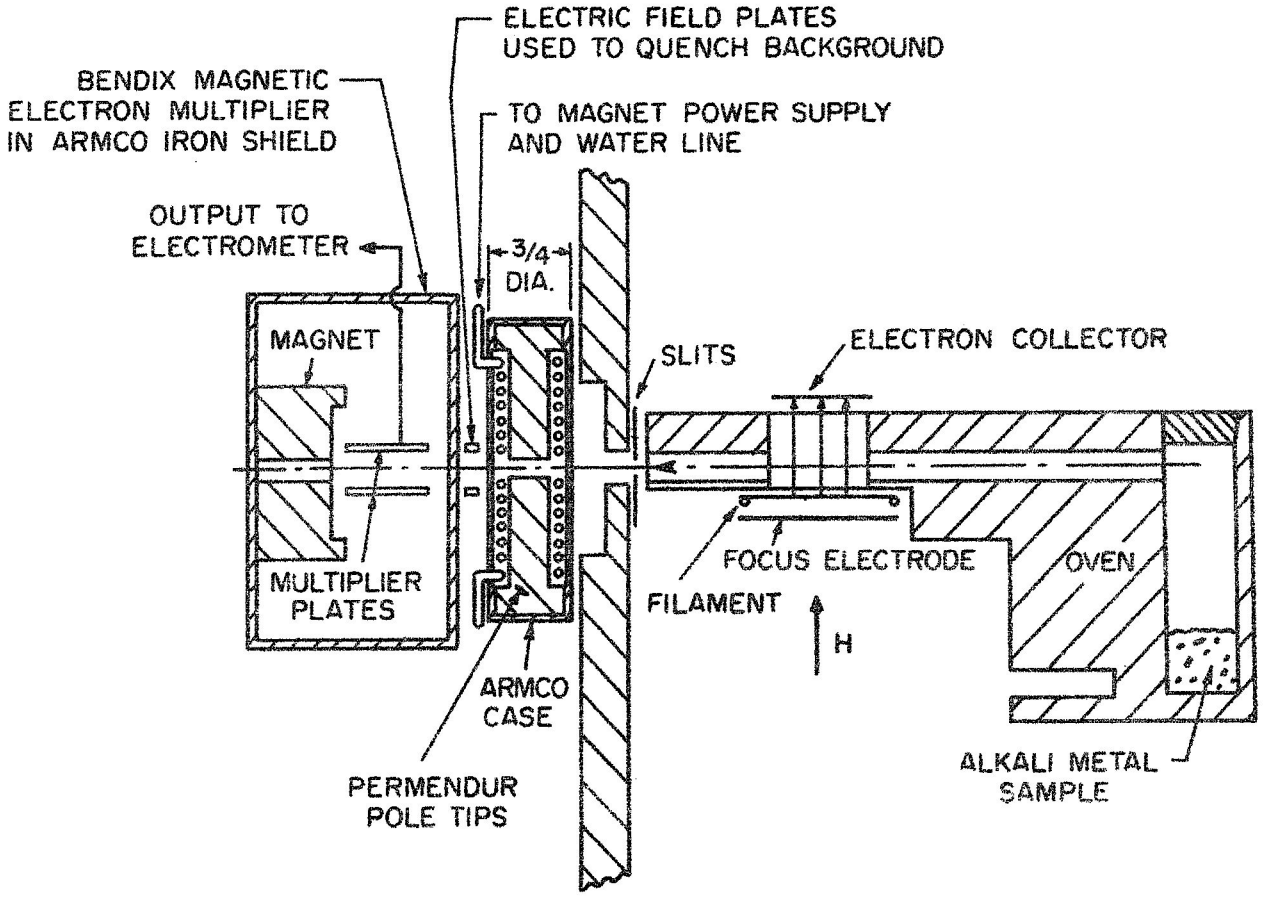

Figure 1. Schematic diagram of the first Zeeman quenching atomic beam apparatus (ref. 8).

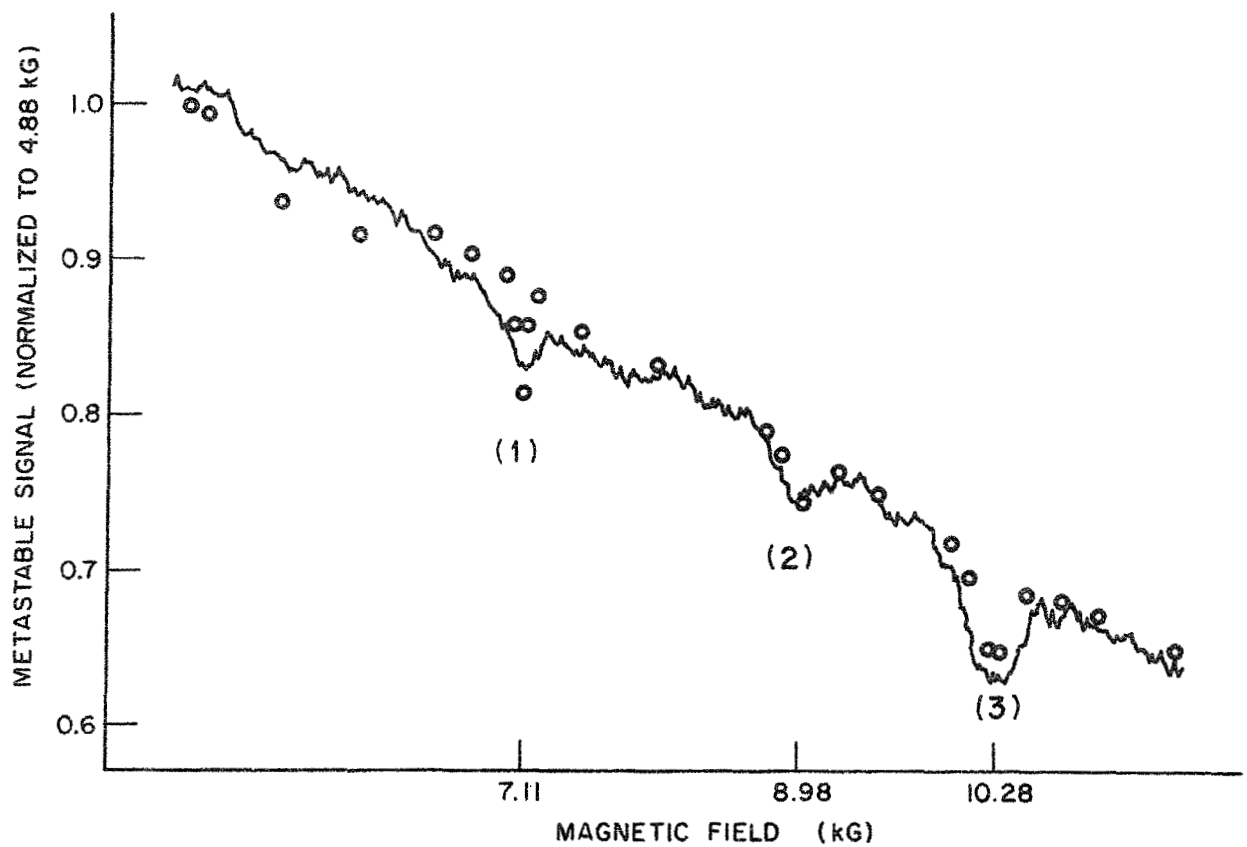

Figure 2. Typical data for Li^7 showing dips in the Zeeman quenching curve. These and similar features in Li^6 were studied in greater detail by signal-averaging techniques (ref. 7).

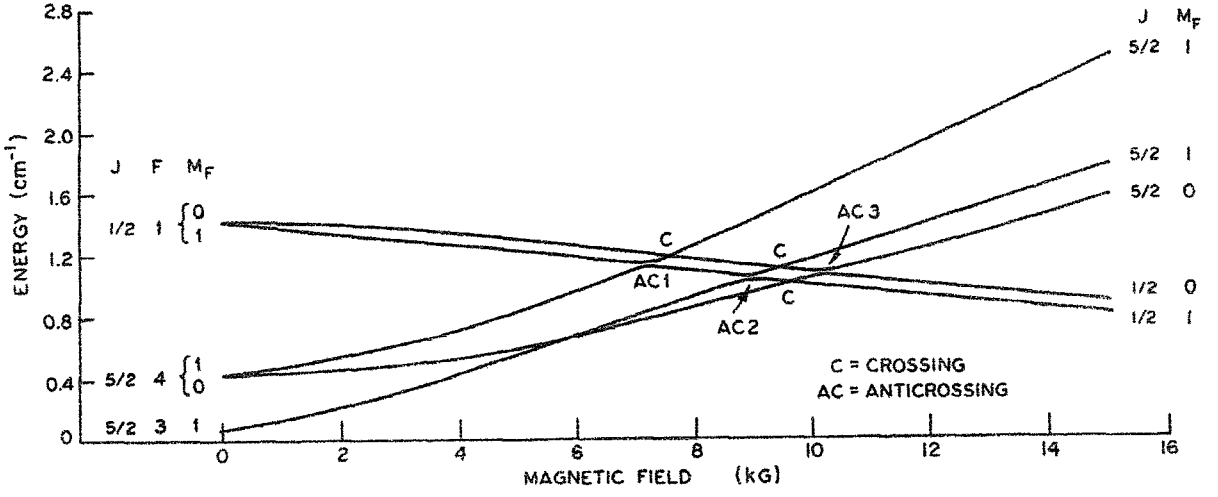

Figure 3. Anticrossings in Li^7 energy diagram responsible for dips in figure 2 (ref. 9).

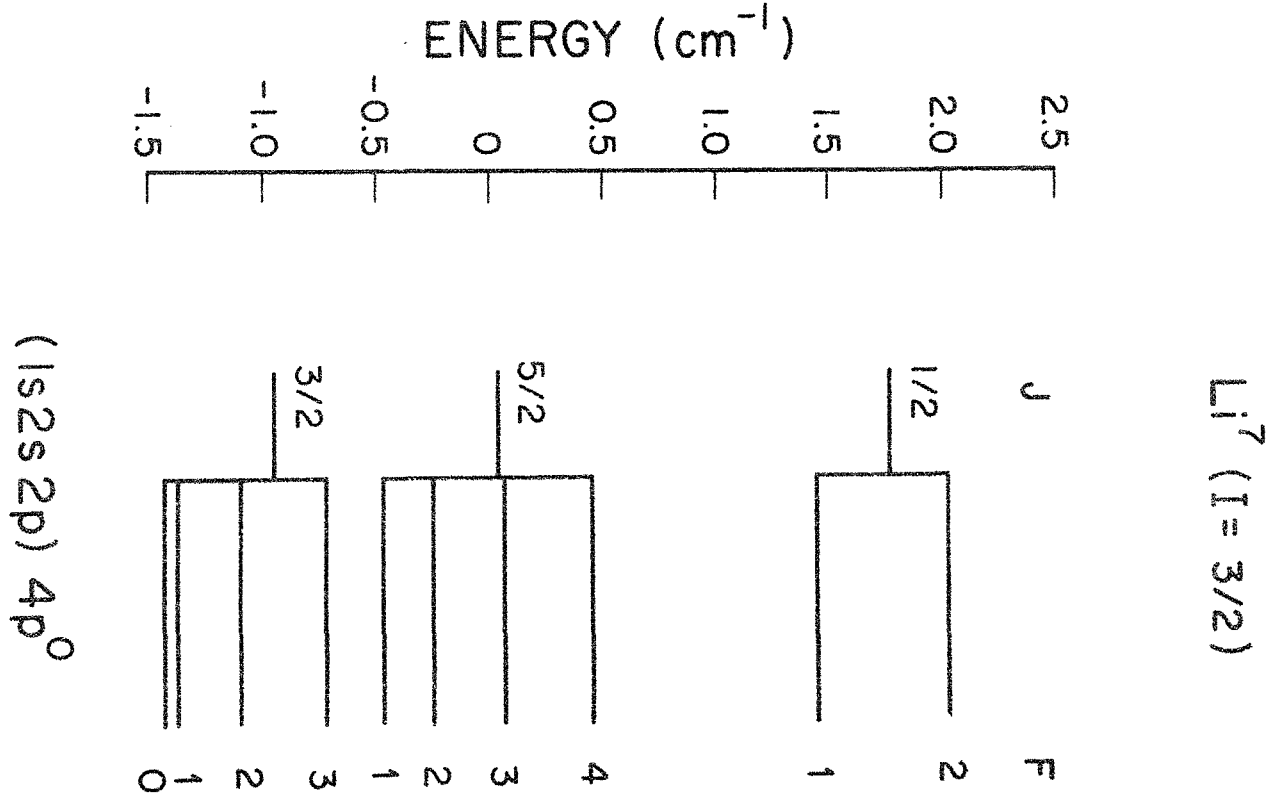

Figure 4. Experimental level diagram for Li^7 (ref. 7).

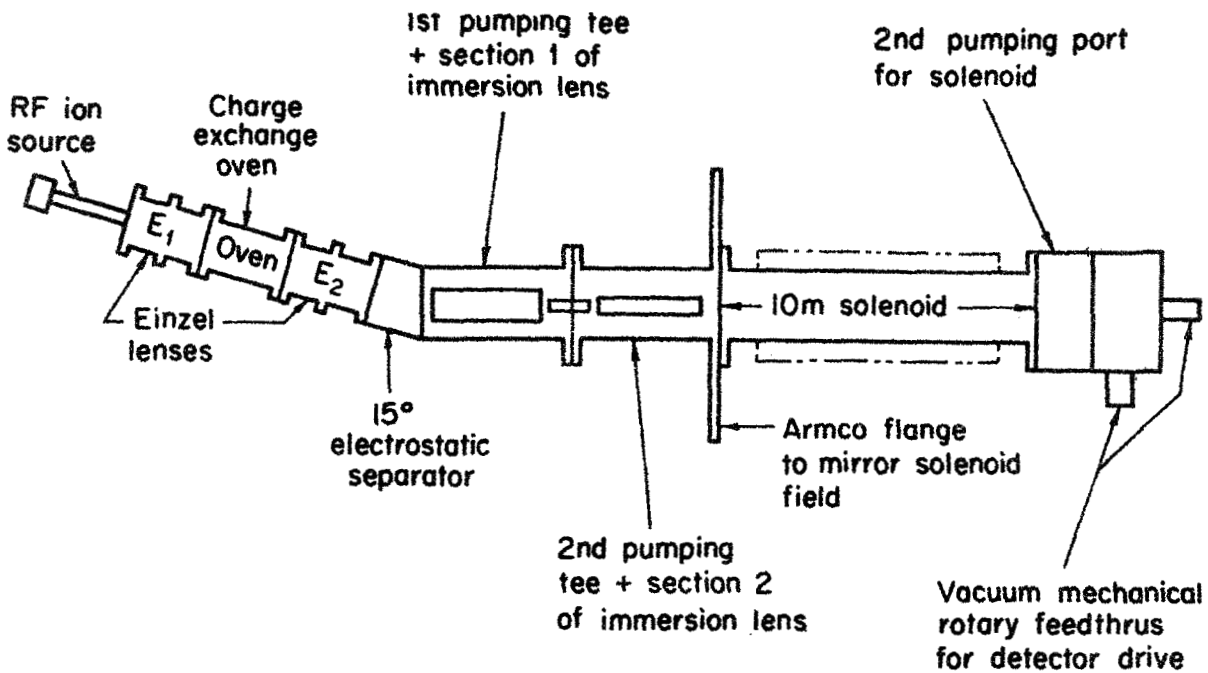

Figure 5. Schematic diagram of the He^- source and detection regions (ref. 12).

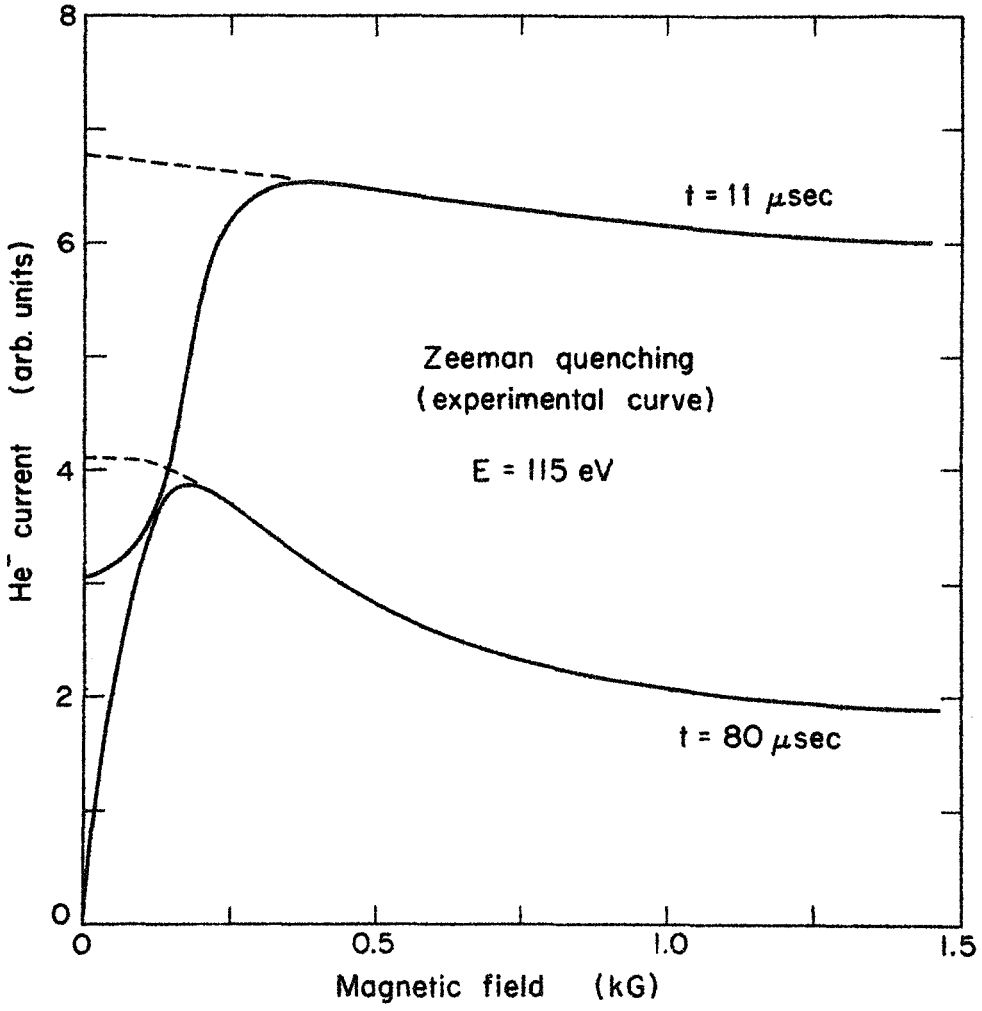

Figure 6. Zeeman quenching of He^- at two flight times. The metastable current drops at low fields because of solid angle losses incurred when the beam is not contained by a magnetic field. The dashed lines represent extrapolation assuming quadratic dependence on the field.

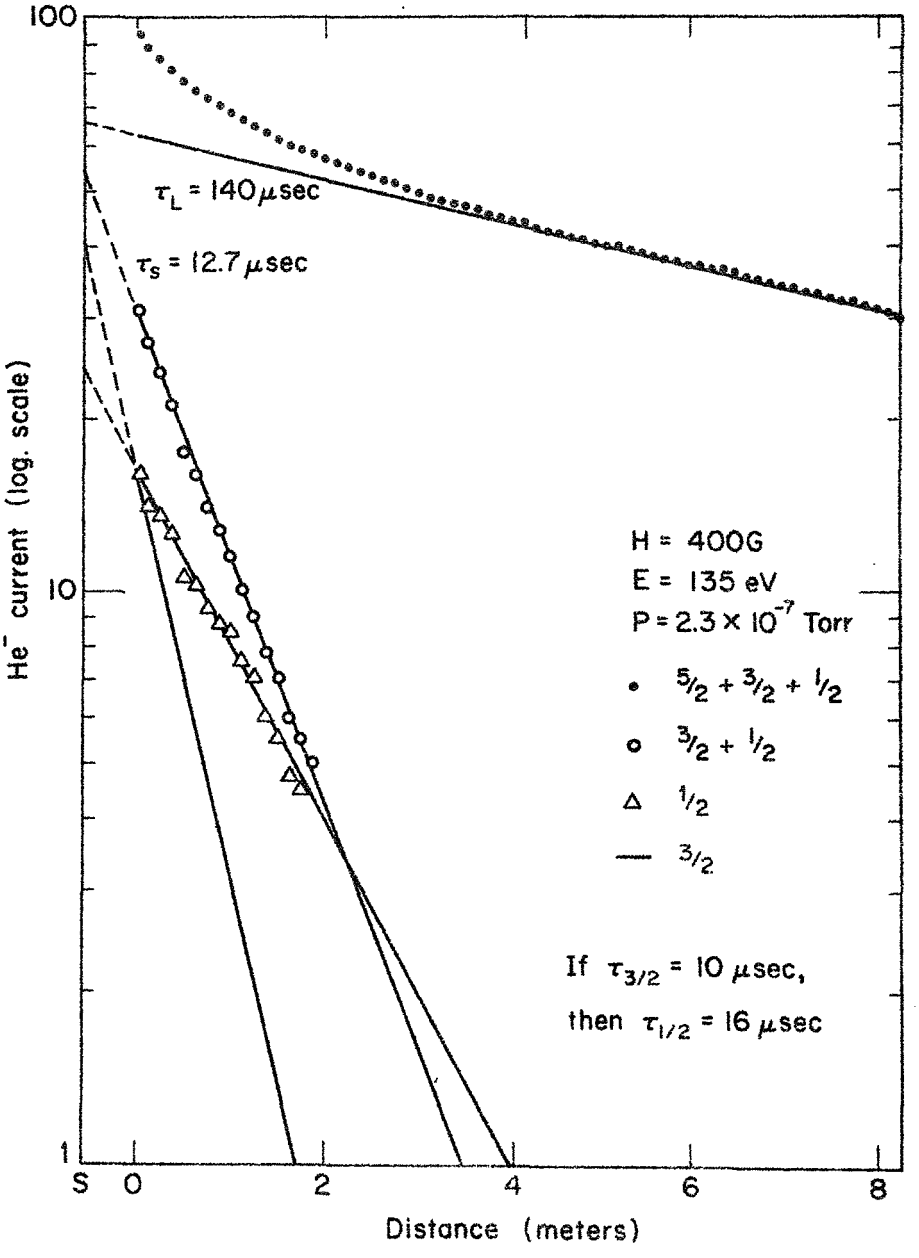

Figure 7. He^- time-of-flight data fitted with two and then three exponential components. The two-component fit (circles and dots) is based on these data alone. The three-component fit uses $\tau_{3/2}$ from Zeeman quenching (fig. 6) to determine $\tau_{1/2}$ (triangles). The relative strengths of the three components extrapolated back to the source at S agree with the statistical weights of the assigned J-states.

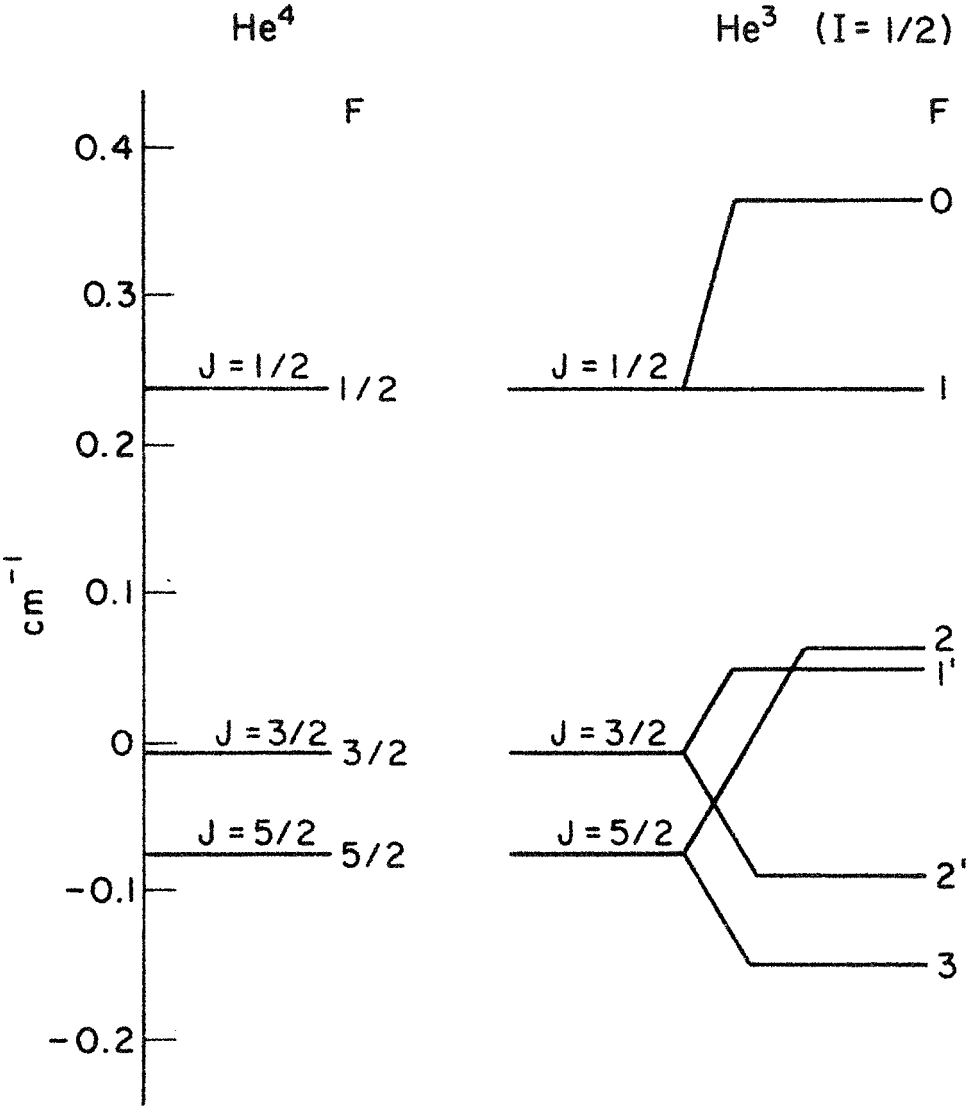

Figure 8. Calculated energy level diagrams for the helium negative ion of the isotopes He^4 and He^3 (ref. 14). A preliminary value (ref. 12) for the $^4P_{5/2}$-$^4P_{3/2}$ splitting is approximately half the calculated value (see table 2). The He^3 states marked 1' and 2' have J = 3/2 weight of 90% and hence are longer-lived than the states marked 2 and 3.

Spectrum of the Two-Photon Emission from the Metastable State of Singly Ionized Helium*

C. J. Artura
Columbia Radiation Laboratory, Department of Physics
Columbia University, New York, New York 10027

R. Novick†
Columbia Laboratory for Astrophysics and Space Physics
Columbia University, New York, New York 10027

N. Tolk
Bell Telephone Laboratories, Inc., Whippany, New Jersey 07981

Verification has been made of the theoretically predicted spectral distribution of the two-photon emission from the metastable $2^2S_{1/2}$ state of singly ionized helium by means of a broadband spectroscopic coincidence counting technique.

We report here on the observation by means of a broadband spectroscopic coincidence counting technique of the spectral distribution of the two-photon emission from the metastable $2^2S_{1/2}$ state of singly ionized helium. Spitzer and Greenstein (1951) suggested that the two-photon emission from metastable hydrogen atoms might make an important contribution to the continuous emission spectra of planetary nebulae. However, it is not the only

---

*This work was supported in part by the Joint Services Electronics Program (U. S. Army, U. S. Navy, and U. S. Air Force under Contract DA-28-043 AMC-00099(E), in part by the National Aeronautics and Space Administration under Grant NGR 33-008-009, and in part by the Office of Naval Research under Contract N00014-67-A-0108-0002. This is CAL contribution No. 6.

†Alfred P. Sloan Research Fellow.

source of planetary continua; other sources include the recombination spectra of hydrogen and helium and free-free transitions. The continua of various planetary nebulae have been measured by several observers (Aller, 1941; Page, 1942; Barbier and Andrillat, 1954; Minkowski and Aller, 1956). Unfortunately, these measurements are not in good agreement, and they do not provide either a test of the theoretically predicted spectral distribution of the two-photon emission from the metastable state of atomic hydrogen or an indication of the extent to which this process contributes to the continua. Since most of the two-photon spectrum lies in the ultraviolet, it may be possible to obtain better measurements with the OAO. No previous laboratory observations are reported of the spectrum of the two-photon decay of metastable hydrogenic atoms, although the observation of a peak in the continuum emission from a hot plasma containing neon has been attributed to the two-photon emission from the metastable 2^1S state of helium-like neon IX (Elton, Palumbo, and Griem, 1968). The two-photon decay of metastable He^+ has been firmly established (Lipeles, Novick, and Tolk, 1965). Attempts to detect similar two-photon decays in excited nuclei have not proved as fruitful (Alburger and Parker, 1964). However, numerous observations have been made of induced two-photon absorption and two-photon emission processes.[1] (Abella, 1962; Kaiser and Garrett, 1961;

1. The work on induced optical two-photon processes always involves the use of a laser source, and the induced photon is necessarily of well-defined frequency.

Hall, Robenson, and Branscomb, 1965; McMahon, Soret, and Franklin, 1965; Salwen, 1955; Strome, 1968; Eisenthal, Dowley, and Peticolas,

1968; Mahan, 1968; Fröhlich and Staginnus, 1967; and Yatsio, Rokni, and Barak, 1968.)

In the nonrelativistic limit, the decay of the hydrogenic $2^2S_{1/2}$ state to the $1^2S_{1/2}$ ground state by means of a one-photon radiative transition is completely forbidden. Relativistic effects allow the $2S \rightarrow 1S$ one-photon magnetic dipole transition, but this is many orders of magnitude weaker than the $2S \rightarrow 1S$ two-photon electric dipole transition. Theoretical estimates by Breit and Teller (1940) indicate that the dominant mode of decay for this metastable state is two-photon emission to the ground state with a decay rate given by $\gamma = 526.464\ \text{sec}^{-1}$, which corresponds to a lifetime of 1.9 msec.[2]

---

2. The hydrogenic atom has one metastable state. On the other hand, the helium-like atom has two metastable states, the 2^1S_0 and the 2^3S_1 states, both of which may decay to the ground state by means of two-photon emission. Two-photon emission is the dominant decay mode of the 2^1S_0 state of helium; however, it is not the dominant decay mode of the 2^3S_1 state of helium. For this state, it has been shown that the lifetime against the one-photon magnetic dipole transition to the ground state is 10^5 sec (Schwartz, 1968), whereas the lifetime against the two-photon decay is 2.2×10^8 sec (Dalgarno, 1968a). As in the case of the hydrogenic metastable state, the two-photon decay rate of the metastable 2^1S_0 state of the helium-like atom has a Z^6 dependence on the nuclear charge. On the other hand, the two-photon decay rate of the metastable 2^3S_1 state of the helium-like atom has been calculated and shown to vary as Z^{10} along the isoelectronic sequence (Bely and Faucher, 1969).

Theory predicts that these photons have a continuous distribution of energy that is both broadly peaked at and symmetric about 20.4 eV (608 Å). [The theoretically predicted spectral distributions of the two-photon emission from both the hydrogenic metastable $2^2S_{1/2}$

state and the helium-like metastable 2^1S_0 state have their maxima when the two emitted photons have the same frequency. However, the theoretically predicted spectral distribution of the two-photon emission from the helium-like metastable 2^3S_1 state is identically zero when the two emitted photons have the same frequency, and has two maxima, one on each side of $\nu_{12}/2$, where $h\nu_{12}$ is the transition energy (Dalgarno, 1968b).] Conservation of energy requires $\nu_1 + \nu_2 = \nu_0$, where ν_1 and ν_2 are the frequencies of the two photons and ν_0 is the frequency corresponding to the difference in energy of the 1S and 2S levels. One photon must lie in the range $\nu = 0$ to $\nu = \nu_0/2$, and the complementary photon must be emitted in the range $\nu_0/2$ to ν_0. Thus the spectral distribution must be symmetric about $\nu_0/2$ when plotted on a frequency scale. Figure 1 shows the theoretically predicted spectral distribution of the two-photon decay plotted on a wavelength scale. We detect the two-photon decay mode by a 15-nsec resolving time coincidence technique, i.e., by simultaneously detecting both photons of the decay. It is inadequate to detect only one-photon events since radiation also results from the excitation of the background gas.[3]

The experimental apparatus, which consists of an electron-bombardment ion source, differential pumping chambers for pressure reduction, and a detection chamber with two phototubes located in a plane perpendicular to the axis of the beam, and the experimental

---

3. In the course of studying the two-photon spectrum using single-photon counting techniques, radiation due to the impact of low-energy metastable singly ionized helium on helium and on the other rare gases has been detected. This is the first experimental study of very low-energy ion-atom excitation where one of the collision partners is initially in an excited state. The results of this preliminary study will be presented elsewhere.

procedure are similar to those employed by Lipeles et al. (1965). However, our present system incorporates several significant improvements over that of Lipeles et al. (1965). We installed a new ion source, similar to that described by Dworetsky, Novick, Smith, and Tolk (1968), which produces an ion beam more than a full order of magnitude greater than that used previously. Installation of additional electrostatic ion lenses has improved the focusing of the beam into the detection region.

The two-photon decay is proportional to $(\hat{e}_1 \cdot \hat{e}_2)^2$, where $\hat{e}_1$ and $\hat{e}_2$ are the polarization vectors of the two photons. Averaging over the polarizations of both photons yields a $(1+\cos^2\theta)$ angular distribution, where θ is the angle between the propagation vectors of the two photons. Thus, with photodetectors insensitive to the polarization of the photons, a $(1+\cos^2\theta)$ angular correlation is predicted for the coincidence counting rate. Lipeles et al. (1965) previously measured the coincidence signal as a function of the angle between two EMI "hard" uv windowless multipliers, which detect photons in the range from 300 to 1200 Å with an average quantum efficiency of about 10%. They thereby verified the $(1+\cos^2\theta)$ angular correlation. In addition to the angular correlation, they measured the dependence of the singles and coincidence counting rates on electron bombarding energy and rf quenching power.[4] Both of the excitation curves showed the expected threshold at 65 eV, the energy needed for the formation of the 2S state of He^+ from

4. The radio-frequency quenching of the $2^2S_{1/2}$ state is accomplished by allowing the ion beam to pass through a microwave field whose frequency corresponds to that of the $2^2S_{1/2} - 2^2P_{1/2}$ transition of He^+ (i.e., the Lamb shift frequency).

the ground state of neutral helium. Furthermore, the rf quenching curves showed the expected exponential dependence of metastable intensity on rf power.

With our improved system we remeasured the angular correlation with the two "hard" uv phototubes. The results of these measurements, shown in Fig. 2, verify the theoretical angular correlation. The solid curve in the figure represents the expected angular distribution after we integrate the $(1 + \cos^2\theta)$ angular factor over the area of the photomultiplier cathodes and over the length of the ion beam exposed to the phototubes. The angular correlation was also measured with one "hard" uv phototube and one EMR 541-F "soft" uv phototube with a LiF window, which is sensitive from 1050 to 3500 Å. This again confirmed the theoretical angular distribution but this time one of the phototubes (the "soft" one) necessarily responded only to photons whose frequency was less than half of the transition frequency. In order to study the spectral distribution of the decay photons, we placed various broadband filters over the face of the "soft" uv phototube. These filters, which include MgF_2, CaF_2, SrF_2, BaF_2, sapphire, and Suprasil (fused silica), have various low-wavelength cutoff limits and transmission characteristics. The coincidence counting rates with the various filters give us information about the two-photon spectral distribution. Table I presents the data obtained.

In Table I, S/S_o is the ratio of the single-photon counting rate with a specific filter to that with no filter; R/R_o is the ratio of the coincidence counting rate with a specific filter to that with no filter. Columns 3 and 4 give the experimental

values for singles and coincidences with their corresponding uncertainties. Columns 5 and 6 give the singles and coincidence values computed from the theoretical expressions for S/S_o and R/R_o, where ν_1 and ν_2 are the frequencies corresponding to the wavelengths of 3500 and 1050 Å, respectively, and ν_3 is the frequency corresponding to the low-wavelength cutoff limit of the specific filter. $T(\nu)$ is the transmission of the filter, η is the efficiency of the "soft" tube, η' is the efficiency of the "hard" tube, and $A(\nu)$ is the two-photon spectral distribution, which has been carefully calculated (to within 0.5%) by Spitzer and Greenstein (1951) as well as more recently and more accurately (to within one part in 10^6) by Klarsfeld (1969).

We have chosen to present the comparison between experimental and theoretical results in terms of the ratios of counting rates rather than in terms of absolute counting rates. This eliminates the effect of frequency-independent quantities, some of which are complicated, difficult to calculate, and not very well understood. With the improved techniques employed here, typical values of S_o for the single rates were 1200 and 200 counts per second for the "hard" and "soft" phototubes, respectively. The coincidence rates were 6 counts per minute for both phototube combinations. The chance coincidence rate was approximately one count per minute with the two "hard" phototubes.

Table I shows that the theoretical relative coincidence counting rates agree with the experimental relative coincidence counting rates. On the other hand, the singles counting rates

show no such agreement since as discussed above there are other sources of single-photon decays.

In order to test the sensitivity of the experiment to the spectral distribution of the two-photon emission, the ratios S/S_o and R/R_o have also been calculated using five other spectral distribution functions $A(\nu)$. The simplest test spectrum to consider is a uniform spectral distribution. This distribution, denoted as $A_{flat}(\nu)$, is independent of frequency and has the form $A_{flat}(\nu) = 1$ for $0 \leq \nu \leq \nu_o$. The second test spectrum $A(\nu^3)$ is defined as proportional to the cube of the product of the frequencies of the two photons, i.e., $A(\nu^3) \propto \nu^3(\nu_o - \nu)^3$. Such a distribution results from considering only the phase space factor in the theoretically predicted two-photon spectral distribution, $A_{normal}(\nu)$, and neglecting the matrix element factor. The third test spectrum to be considered, the reverse spectrum, is obtained by reflecting the theoretically predicted spectrum about $\nu_o/4$ for $0 \leq \nu \leq \nu_o/2$ and about $3\nu_o/4$ for $\nu_o/2 \leq \nu \leq \nu_o$. Therefore, $A_{reverse}(\nu) = A_{normal}[(\nu_o/2) - \nu]$ for $0 \leq \nu \leq \nu_o/2$. The final test spectra are $A_{singlet}(\nu)$ and $A_{triplet}(\nu)$, which are the theoretically predicted spectral distributions of the two-photon emission from the metastable 2^1S and 2^3S states, respectively, of the helium atom (Dalgarno, 1968a). All of these spectral distributions are symmetric about $\nu_o/2$ and are defined as zero outside the interval $0 \leq \nu \leq \nu_o$. The results of these calculations are presented in Table II. The values of R/R_o calculated with these various spectral distributions fall within the uncertainties of the experimental values except for those obtained with the following filters: Suprasil in the

case of the flat spectrum; strontium fluoride and calcium fluoride in the case of the ν^3 spectrum; Suprasil in the case of the reverse spectrum; and sapphire and Suprasil in the case of the triplet spectrum. The values calculated using the theoretically predicted (normal) spectrum are in good agreement with the experimental values in all cases.

As discussed above, energy conservation requires that in the two-photon decay one photon have a wavelength lying between 304 and 608 Å and the complementary photon have a wavelength greater than 608 Å. Since the "soft" phototube is sensitive from 1050 to 3500 Å, two such "soft" phototubes cannot detect a true two-photon coincidence. To verify that indeed there are no "soft"-"soft" coincidences, we set two "soft" phototubes at an angular separation of 120° and looked for coincidences between these two tubes. Since cosmic rays produce a troublesome coincidence background, we surround each phototube with a concentric cylindrical shell of plastic scintillator which acts as an anticoincidence shield against cosmic rays. "Soft"-"soft" coincidences are accepted but "soft"-"soft" scintillator triple coincidences are rejected. This procedure reduced the coincidence background from about 10 to 3 counts/min. The residual background is believed to result from the pickup of electrical transients in the laboratory.

By collecting data for 62 hours, we established an upper limit of 0.04 counts per minute for the "soft"-"soft" coincidence, i.e., the rate is less than 0.04 counts per minute. This limit was determined by the fluctuations in the chance coincidence rate and the residual instrumental coincidence rate. To get some

idea of the significance of this quantity, we compare it with both the "hard"-"soft" and "hard"-"hard" coincidence rates, each of which is typically six counts per minute. Thus we have shown that the "soft"-"soft" coincidence rate is at least a factor of 150 smaller than the observed coincidence rates and that our observations are consistent with the theoretical prediction of a zero rate for this quantity.

All of the tests that we have performed here and previously (Lipeles et al., 1965) indicate that the $2^2S_{1/2}$ state of He^+ decays by two-photon emission as predicted by Breit and Teller. We have shown that photon coincidences are observed when and only when metastable ions are present in the ion beam, that the angular correlation function for the coincidences agrees with the theoretically expected function $(1+\cos^2\theta)$, and that the spectrum of the photons is consistent with the predicted spectrum. In making the spectral studies, we were limited to the use of broadband filter techniques because the coincident counting rate was so small. However, the spectral studies certainly show that the spectrum is continuous and that the coincident pairs of photons do not both lie in the spectral range from 1050 to 3500 Å. We believe that our observations firmly establish the two-photon nature of the decay in all essential details and that the theory is reliable and can be applied to the study of planetary nebulae and related astrophysical phenomena.

TABLE I. Comparison of experimental and theoretical results for the two-photon spectrum

Relative singles and coincidence rates with filters

Filter	Cutoff	S/S_o	R/R_o	S/S_o	R/R_o
		Experimental	Experimental	Theoretical	Theoretical
MgF_2	1130 Å	0.7128 ± 0.0051	0.63 ± 0.15	0.697	0.696
CaF_2	1225 Å	0.6633 ± 0.0049	0.60 ± 0.15	0.570	0.569
SrF_2	1275 Å	0.6451 ± 0.0051	0.61 ± 0.16	0.529	0.528
BaF_2	1325 Å	0.6709 ± 0.0049	0.48 ± 0.14	0.5045	0.5046
Sapphire	1425 Å	0.5334 ± 0.0044	0.46 ± 0.12	0.491	0.493
Suprasil	1600 Å	0.4749 ± 0.0042	0.32 ± 0.12	0.423	0.419

$$\frac{S}{S_o} = \frac{\int_{\nu_1}^{\nu_3} T(\nu)\eta(\nu)A(\nu)\,d\nu}{\int_{\nu_1}^{\nu_2} \eta(\nu)A(\nu)\,d\nu}, \quad \frac{R}{R_o} = \frac{\int_{\nu_1}^{\nu_3} T(\nu)\eta(\nu)\eta'(\nu_o - \nu)A(\nu)\,d\nu}{\int_{\nu_1}^{\nu_2} \eta(\nu)\eta'(\nu_o - \nu)A(\nu)\,d\nu}$$

$\nu_1 = (3500\ \text{Å})$, $\nu_2 = (1050\ \text{Å})$, $\nu_3 = (\text{Filter Cutoff})$

TABLE II. Sensitivity of experimental results to various spectral distributions.

EMI-EMR relative coincidence rates with filters

Filter	R/R_o						
	Experimental Results	Calculated Results					
		Normal	Flat	$\nu^3(\nu_o-\nu)^3$	Reverse	He $I(2^1S)$[b]	He $I(2^3S)$[b]
MgF_2	0.63 ± 0.15	0.696	0.718	0.608	0.726	0.684	0.755
CaF_2	0.60 ± 0.15	0.569	0.600	0.448[a]	0.611	0.553	0.651
SrF_2	0.61 ± 0.16	0.528	0.561	0.400[a]	0.572	0.511	0.614
BaF_2	0.48 ± 0.14	0.5046	0.543	0.358	0.555	0.485	0.604
Sapphire	0.46 ± 0.12	0.493	0.529	0.348	0.541	0.474	0.589[a]
Suprasil	0.32 ± 0.12	0.419	0.466[a]	0.253	0.480[a]	0.396	0.535[a]

a. Indicates lack of agreement between experimental and calculated values.

b. These have been scaled to correspond to the $1^2S_{1/2} - 2^2S_{1/2}$ transition in He^+.

REFERENCES

Abella, I. D. 1962, Phys. Rev. Letters, 9, 453.

Alburger, D. E. and Parker, P. D. 1964, Phys. Rev., 135, B294.

Aller, L. H. 1941, Ap. J., 93, 236.

Barbier, D. and Andrillat, H. 1954, Compt. Rend., 239, 1099.

Bely, O. and Faucher, P. 1969, Astron. Astrophys., 1, 37.

Breit, G. and Teller, E. 1940, Ap. J., 91, 215.

Dalgarno, A. 1968a, private communication.

_____ 1968b, in International Conference on Atomic Physics Abstracts, eds. V. W. Cohen and G. zuPutlitz, (New York University, 3-7 June), p. 46.

Dworetsky, S., Novick, R., Smith, W. W., and Tolk, N. 1968, Rev. Sci. Instr., 39, 1721.

Eisenthal, K. B., Dowley, M. W., and Peticolas, W. L. 1968, Phys. Rev. Letters, 20, 93.

Elton, R. C., Palumbo, L. J., and Griem, H. R. 1968, Phys. Rev. Letters, 20, 783.

Fröhlich, D. and Staginnus, B. 1967, Phys. Rev. Letters, 19, 496.

Hall, J. L., Robenson, E. J., and Branscomb, L. M. 1965, Phys. Rev. Letters, 14, 1013.

Kaiser, W. and Garrett, C. G. B. 1961, Phys. Rev. Letters, 7, 229.

Klarsfeld, S. 1969, private communication.

Lipeles, M., Novick, R., and Tolk, N. 1965, Phys. Rev. Letters, 15, 690.

Mahan, G. D. 1968, Phys. Rev. Letters, 20, 332.

McMahon, D. H., Soret, R. A., and Franklin, A. R. 1965, Phys. Rev. Letters, 14, 1060.

Minkowski, R. and Aller, L. H. 1956, Ap. J., 124, 93.

Page, T. L. 1942, Ap. J., 96, 78.

Salwen, H. 1955, Phys. Rev., 99, 1274.

Schwartz, C. L., private communication reported in M. Steinberg, Ph.D. Thesis, University of California (Berkeley), 1968 (unpublished).

Spitzer, L., Jr. and Greenstein, J. L. 1951, Ap. J., 114, 407.

Strome, F. C., Jr. 1968, Phys. Rev. Letters, 20, 3.

Yatsio, S., Rokni, M., and Barak, S. 1968, Phys. Rev. Letters, 20, 1282.

FIGURE CAPTIONS

Fig. 1. Predicted two-photon spectrum for He^+ on a wavelength scale.

Fig. 2. Observed angular distribution of two-photon decay.

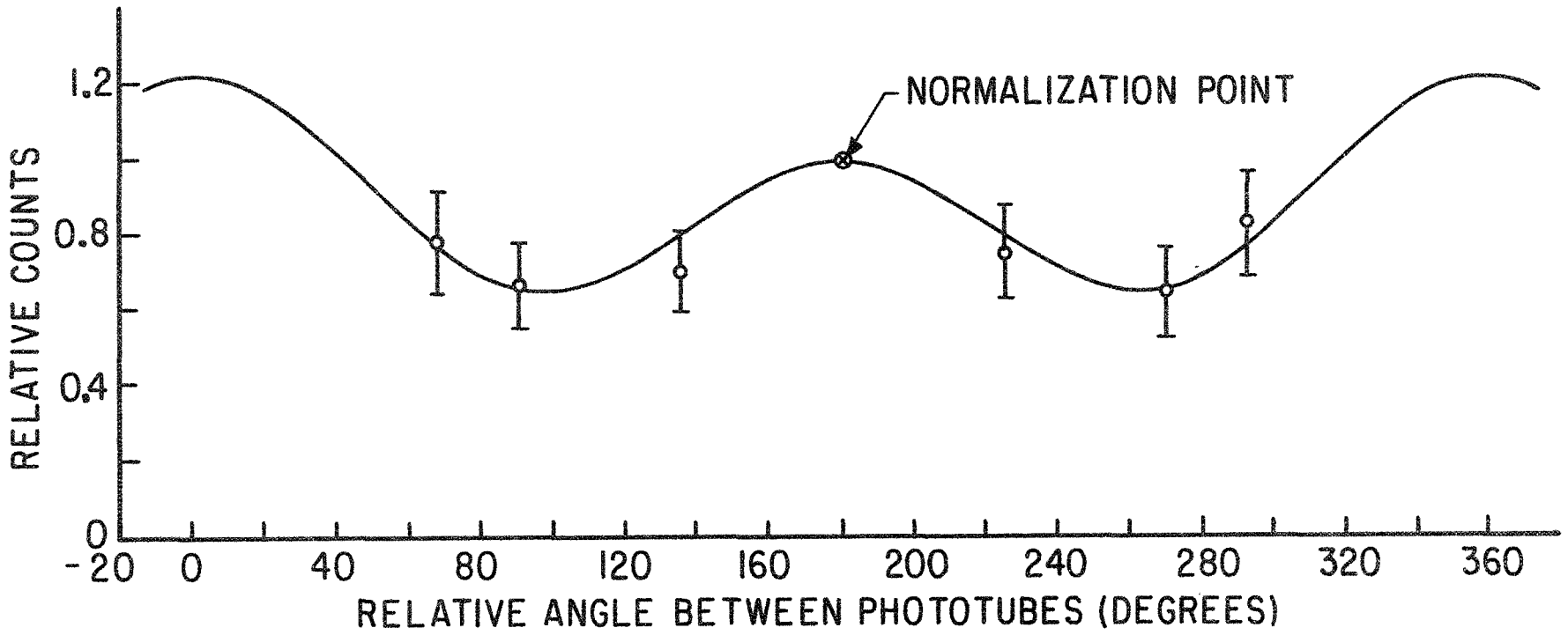
NORMALIZATION POINT
RELATIVE COUNTS
1.2
0.8
0.4
0
-20
0
40
80
120
160
200
240
280
320
360
RELATIVE ANGLE BETWEEN PHOTOTUBES (DEGREES)

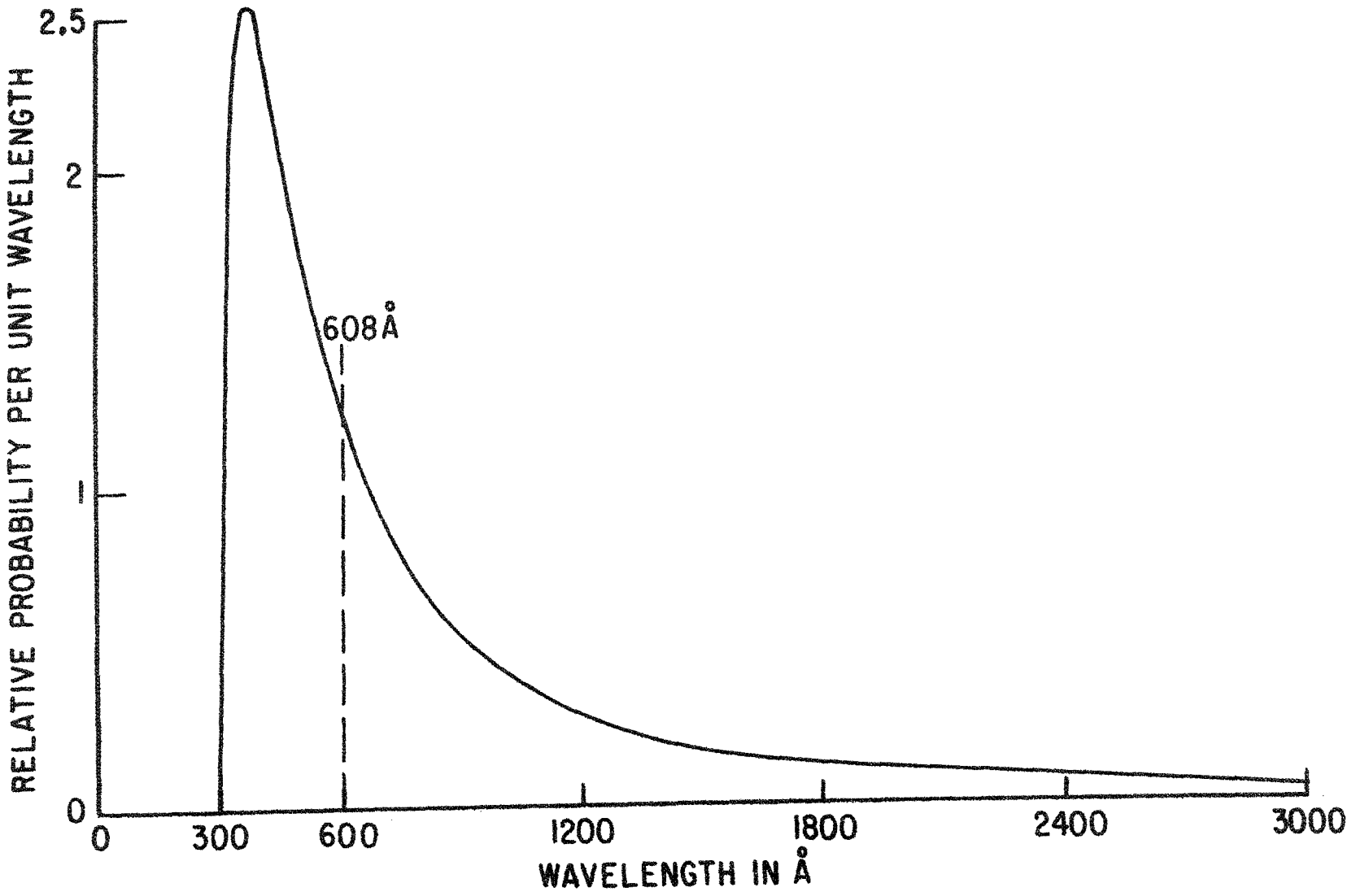
RELATIVE PROBABILITY PER UNIT WAVELENGTH
2.5
2
608Å
0
0
300
600
1200
1800
2400
3000
WAVELENGTH IN Å

Fig. 1